IRAQI BULLETIN OF GEOLOGY AND MINING (IBGM)\
IRAQ GEOLOGICAL SURVEY (GEOSURV-IRAQ)

*IBGM (**2025**, Vol 21; Issue 1)* *275-306*

PRODUCTIVITY ASSESSMENT FOR UNIT A OF THE LATE TRIASSIC KURRA CHINE FORMATION FROM A WELL IN THE BINA BAWI OILFIELD, IRAQI KURDISTAN REGION

Dler H. Baban[1*] and Mustafa M. Nanakali[2]

[1] Department of Geology, Sulaimani University, Sulaimaniyah, Kurdistan Region-Iraq.
[2] Department of Petroleum Geosciences, Soran University, Erbil, Kurdistan Region-Iraq; e-mail: geopetrol1995@gmail.com
***** *Corresponding author e-mail: dler.mohamad@univsul.edu.iq*

Type of the Paper (Article)
Received: 02/ 08/ 2024
Accepted: 18/ 02/ 2025
Available online: 27/ 06/ 2025

Abstract

Unit A of the Triassic Kura China Formation has been studied from a productivity assessment point of view in the selected BB-4 well of Bina Bawi Oilfield, Iraqi Kurdistan Region, to identify its productive potential. The study is done based mainly on the available full sets of wireline log data for the gross penetration of 323 m of the unit. The lithology was identified depending on the data from the porosity logs and appeared to be mainly composed of dolomite, anhydritic dolomite, and anhydrite with rare limestones. The data from the Gamma-ray indicated low shale content (less than 10%) at the upper part of the unit, whereas at the middle and lower parts, shale and shale intervals are common. The existing shale in the studied Unit A is mostly distributed as dispersed clay materials between the grains. The porosity of the unit was evaluated depending on the calculated corrected Neutron-Density combination log and showed that the unit is of poor porosity, being on average less than 5%. The permeability in the BB-4 well was obtained from the data of the Nuclear Magnetic Resonance (NMR) log and showed a lot of impermeable or poor permeable horizons. Depending on the differences in the shale volume, porosity, and permeability values, three reservoir units were selected for the unit under study. Hydrocarbons with different saturation percentages exist along Unit A of the Kurra Chine Formation in the studied well, and most of the existing hydrocarbons are non-movable (residual hydrocarbons). The calculated net-to-gross (N/G) reservoir, pay, and productive ratios for the studied Unit A collectively in the well BB-4 appeared to be 9.2%, 3.28%, and 3.28%, respectively.

Keywords: Kurra Chine; Bina Bawi; Reservoir Units; Movable hydrocarbons; Reservoir characterization; productivity.

ISSN 1811-4539, EISSN 3005-3714
https://doi.org/10.59150/ibgm2101a16

1. Introduction

Kurra Chine and Geli Khana formations are two Late Triassic formations in the Kurdistan Region that are thought to be potential reservoirs. The majority of research on the Kurra Chine Formation conducted outside of the Kurdistan Region evaluates the formation as a potential source rock (Sadooni, 1995; Al-Barzingy, 1999; Al-Ameri et al., 2009; Vulama, 2011; Al-Ameri & Zumberge, 2012; and Edilbi et al., 2019). Grunau (1983) and Sadooni (1995)agreed and suggested that the Kurra Chine Formation contains both source and reservoir rocks in northern Iraq. The formation in the northwest part of Iraq, the northwest part of Syria, and the southeast part of Turkey is thought to be a Triassic reservoir for oil and gas, and in the fields of Sfayya, Allan, and Butma in Iraq as well as in Swedia, Rumeilan, Jbesa, and Tishereen fields in Syria, the evaporite beds of the same formation serve as a cap rock for its reservoir portions (Al-Sakini, 1992). According to Mackertich & Samarrai (2015), the Late Triassic Kurra Chine Formation in the Shaikhan Field yielded 11.2 – 20.4 million standard cubic feet of gas and 5,474 barrels of oil daily.

The formation was primarily identified as a reservoir rather than a source by the exploration and drilling operations conducted in the Kurdistan Region in the last two decades. The Kurra Chine Formation in Kurdistan Region is often found at shallower depths and is easier to explore and drill than other areas of Iraq, despite the high reservoir pressure that still presents a significant obstacle. The formation has been drilled as one of the targets or is scheduled to be drilled in several of the recently found oilfields in the Kurdistan Region, such as Swara Tika, Sheikh Adi, Bakrman, Sarta, Atrush, Shaikhan, Simrit, Barda Rash, Mirawa, Shakrok, Bina Bawi, Sangaw, etc.

This study attempts to define the reservoir properties of the upper part of the Kurra Chine Formation (Unit A) using the existing wireline log data from a selected well (BB-4) at Bina Bawi Oilfield.

2. Kurra Chine Formation

The most attractive late Triassic formation in Iraq from a petroleum exploration point of view is the Kurra Chine Formation. Wetzel initially described it in 1950 (Bellen et al., 1959) based on the monotonous dark brown and black limestone found in the northern thrust zone in northern Iraq. The formation, as outlined in its type section at Ora in the Iraqi Kurdistan Region, is primarily made up of dolomites and papery shale interspersed with dark, brown limestones (Dunnington, 1958in Bellen et al., 1959). The formation is composed of alternating limestone, dolomites, shale, and halite at the subsurface, with thick evaporite intervals (Buday, 1980).

The Kurra Chine Formation's depositional habitat is distinguished by lagoonal, occasionally euxinic, conditions in the foothills and Mesopotamian Zone ((Jassim et al., 2006). Shallow subtidal and supratidal cycles with local sabkhas dominate the epeiric platform where the upper carbonate-dominated portion of the formation is deposited (Aqrawi et al., 2010).

The Kurdistan Region's operating oil companies recently divided the formation into three divisions (units), A, B, and C, which represent the upper, middle, and bottom portions of the formation, respectively. The primary geological features of Kurra Chine's unit A are anhydrite strata that are separated by mudstones and dolomites. The upper part of this unit is dominated by mudstone. The Kurra Chine's unit B, on the other hand, is mainly made up of mudstones, particularly in the lower part of this unit, as well as dolomite, dolomitic anhydrite, and anhydrite. Dolomitic anhydrite, limestone, anhydrite, and dolomite make up the majority of the composition of Kurra Chine's unit C.

According to Sadooni & Alsharhan (2004), future hydrocarbon exploration in eastern Syria and northwest Iraq is primarily focused on the Kurra Chine dolomite unit and the Triassic layers in the Euphrates-Anah graben in both countries, which contain reservoir and cap-rock lithologies.

The report of the Ryder Scott Company (2011) mentioned that dolomites, whose porosities are estimated to vary from 7 to 15%, are the main reservoirs in the Kurra Chine Formation in Shaikan Field and that fracturing has increased the permeabilities of the reservoir rocks.

Awdal et al. (2016) classified the Kurra Chine Formation as a type II reservoir, according to Nelson's (2001) categorization of fractured reservoirs, since fractures supply the necessary reservoir permeability while the matrix contributes less.

A map of the Late Triassic deposits in northern Iraq and the corresponding hydrocarbon fluid phases was created by English et al. (2015). They demonstrated that although the Late Triassic source rocks (including the Kurra Chine Formation) in Bina Bawi Field are in the wet gas-condensate generation stage, they are (as source rocks) in Swara Tika and Shaikan fields thermally in the oil generation stage.

Edilbi et al. (2019) have evaluated the shale intervals as source rocks within the Kurra Chine Formation and they have explained that the Total Organic Carbon (TOC wt.%) values for the shale intervals indicate fair to good source rocks related organic matter richness. The kerogen appeared to be a mixed type II-III and III. The maximum recorded temperature values by pyrolysis analysis (T_{max}) display that organic matters of the Kurra Chine Formation are thermally mature and are in the main oil window.

The Kurra Chine Formation's lower and upper reservoir parts are separated in the Alan Field by 220 meters of anhydrite cap rocks (Alhadithi & Al-Hadithy, 2020).

Unit A of the Kurra China Formation in the well of Shaikan-4 (SH-4) from Shaikan Oilfield in the Iraqi Kurdistan Region has been evaluated by Baban & Ahmed (2022). They figured out that Unit A, which represents the upper part of the formation, is of low shale content except at the uppermost part of the unit where the shale content exceeds 30%, and is generally of lower than 5% porosity in most parts of the unit. They also mentioned that almost the whole unit in the well SH-4 contains hydrocarbons in different saturations and exceeds 70% at the middle and lower parts of the unit.

The formation in well Sarta-2 (S-2) in Sarta Oilfield is composed of limestone, dolomite, anhydrite, shale, and sandstone, with an average shale content of about 17%, an average porosity of about 5%, an average permeability of about 30.6 mD, and an average hydrocarbon saturation of about 45% (Aswad et al., 2024).

3. Bina Bawi Oilfield

The Bina Bawi Anticline lies some 40 Km east of the city of Erbil and about 10 Km north of Taq Taq Oilfield (Figure 1A) and covers an area of approximately 88 km^2 on the surface, and is located on the southwestern edge of the Zagros Fold Belt of the Kurdistan Region. The anticline is striking from NW to SE following the trend of the Zagros Mountains with a distinct surface expression (Figure 1B).

The Bina Bawi Anticline is part of a 25 – 50 Km wide belt of imbricates, folds, and faulted folds (High Folded Zagros Zone) that was formed by the Zagros deformation, which was initiated in the Late Cretaceous and had its peak during the Late Cenozoic (Hamood, 2012).

According to the overall structural expression, the anticline is roughly 40 km long and 8 km wide. In the NW, it is replaced by a syncline–anticline pair that leads to the Pirmam Anticline (Awdal et al., 2016). The Bina Bawi anticline is an asymmetrical anticline whose dip of the northeastern limb ranges between 18º and 22º and the southwestern limb between 33º and 45º and forms a left-hand en-echelon plunge with the Taq Taq anticline and right-hand en-echelon plunge with the Pirmam anticline (Ghafur et al., 2023).

The double plunging Bina Bawi anticline is partially bounded by two strike trending faults; one to the NW and one to the SE. The structure is characterized by its long, narrow shape consisting of one main culmination (Dallali, 2013). The anticline's carapace is composed of rocks from the Bekhme and Shiranish formations.

Reservoir zones in the field include Jurassic and Triassic period succession, but it seems clear that the Cretaceous reservoir is not available in the Bina Bawi Oilfield due to lacking the top seal (Figure 2) (Dallali, 2013).

The field's gas-bearing Triassic age layers have an estimated hydrocarbon column of more than 1,000 meters (Mackertich & Samarrai, 2015).

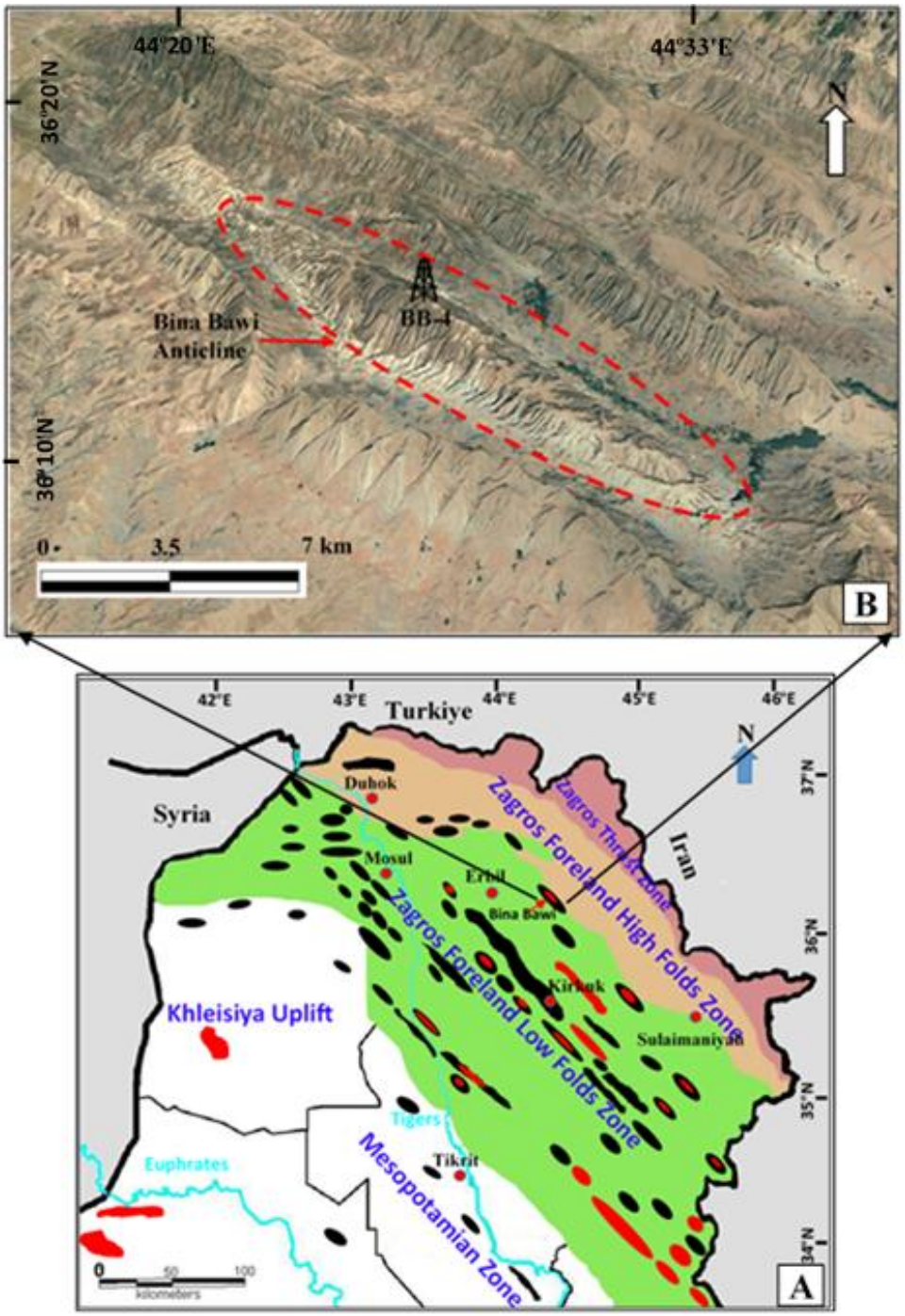

Figure 1. A) Location map of Bina Bawi Oilfield on the Northern Iraqi Tectonic map; B) Location of well BB-4 on the Bina Bawi Anticline (the photo is taken from Google Earth).

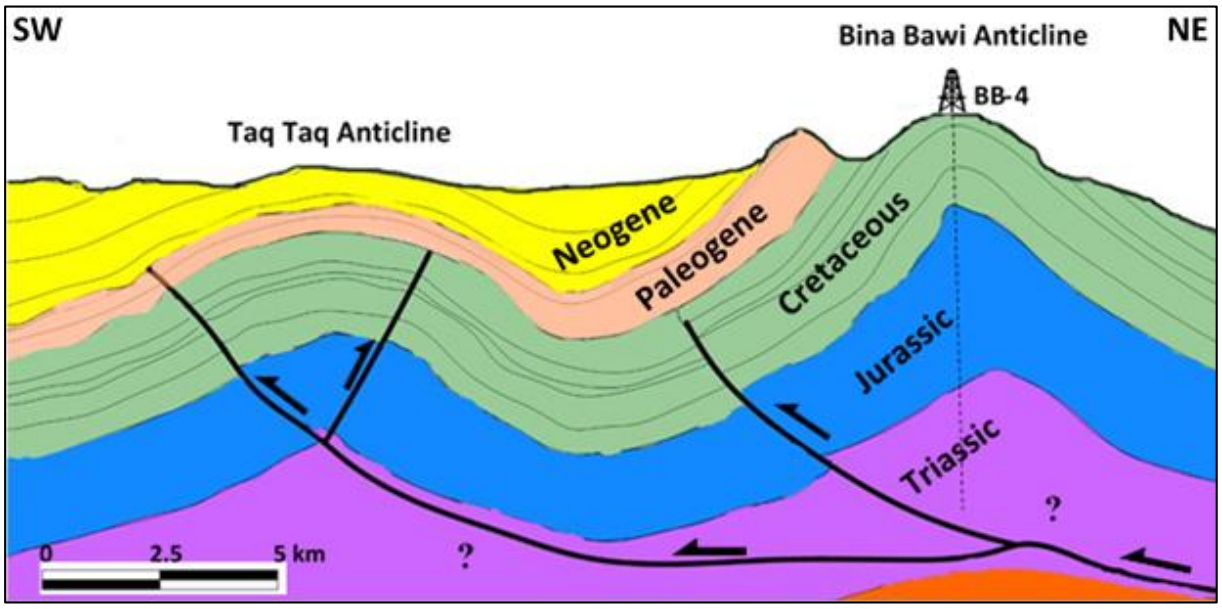

Figure 2. Structural cross-section of the Bina Bawi Oilfield and the nearby Taq Taq anticline showing the penetrated successions by well BB-4 starting at the surface with the Late Cretaceous beds (Aqra-Bakhma Formation) (modified after Hinsch & Bretis (2015).

4. Tectonic Setting and Stratigraphy

The Bina Bawi structure is situated behind the distinct topographic line that divides the sharply rising mountains to the northeast from the lowlands in the southwest. The Mountain Front Flexure/Fault (MFF) is a common name for this boundary, and the Bina Bawi structure is located towards the hinterland of the MFF (Hinsch & Bretis, 2015).

Tectonically, the Bina Bawi anticline is located in the Zagros Foreland High Folds Zone, but in its outermost part, in the Zagros Foreland Low Folds Zone. This upright, slightly asymmetrical, NW – SE trending anticline verges to the SW. It is a moderately dipping forelimb and the Late Cretaceous units are cropped out in the fold crest and as a belt surrounding the anticline hinge (Awdal et al., 2016).

The Neogene and Paleogene formations are completely eroded at the crest and middle part of the Bina Bawi anticline, and they no longer represent part of the trap but just as outcropped beds representing the remaining eroded limbs. Spudding in most of the drilling locations starts with the outcropped Late Cretaceous Aqra/Bakhma Formation. As part of the Zagros Highly Folded Belt, the common feature of missed Oligocene and Early Miocene formations can also be seen in the study area.

The Fat'ha Formation is unconformably rested above the Late Eocene Pila Spi or Avana formations. Figure 3 represents the common stratigraphic column of the study area as suggested by Hinsch & Bretis (2015) based on Aqrawi et al. (2010), Bellen et al. (1959), Cohen et al. (2013), and Zebari (2013).

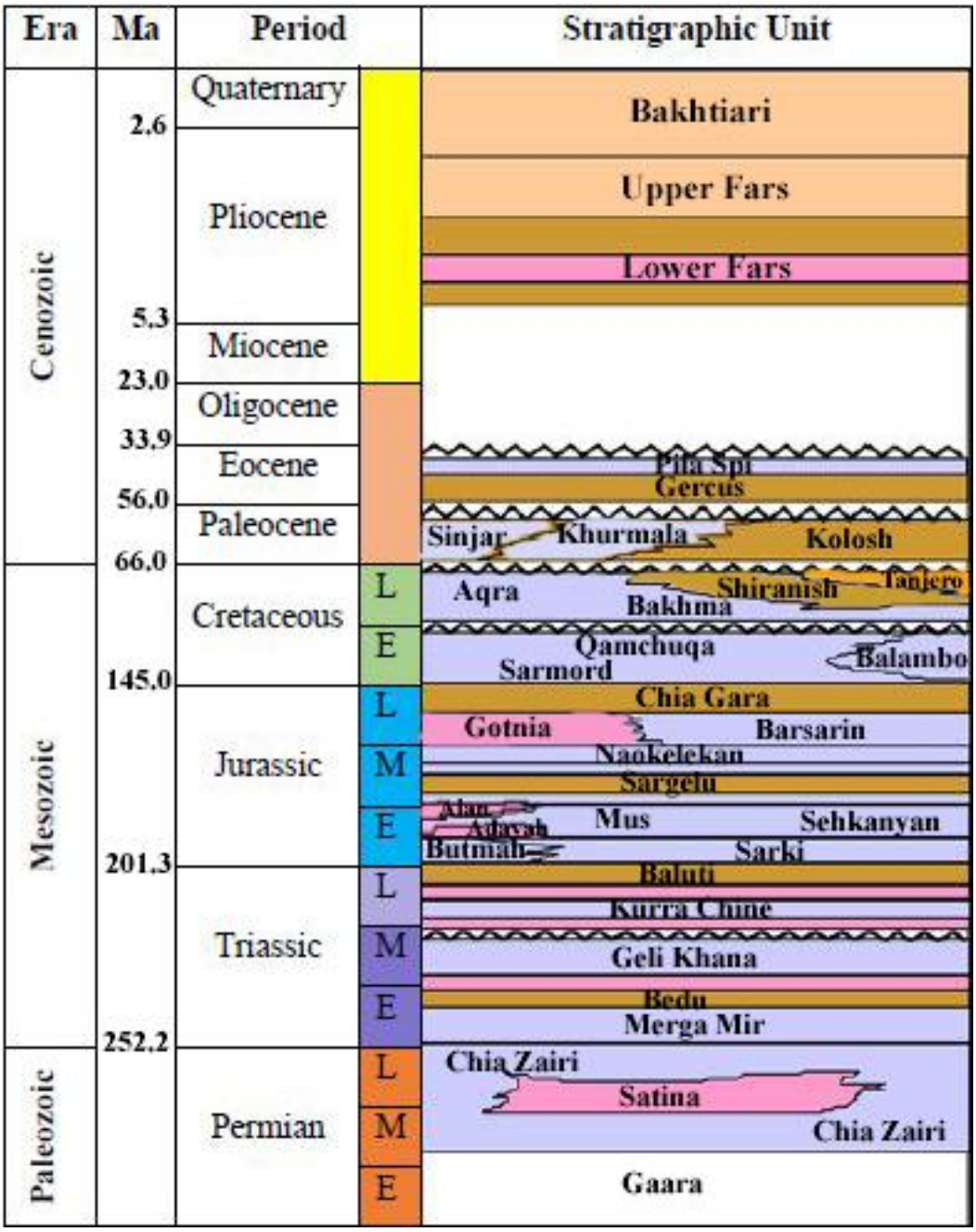

Figure 3. Stratigraphic column for the study area after Hinsch & Bretis (2015) based on data from Aqrawi et al. (2010), Bellen et al. (1959), Cohen et al. (2013), and Zebari (2013) in addition to OMV Oil Company's internal reports.

5. Lithology Determination

Knowing the lithology of the reservoir serves as the basis for all other petrophysical computations. To do correct petrophysical calculations of porosity, water saturation (Sw), and permeability, the number of lithologies of the reservoir interval should be recognized and their implications understood (Hamada, 2013). Many logging tools are available to detect types of lithology for the reservoir beds, such as Gamma-ray logs and porosity logs (Sonic, Density, and Neutron). Generally, a single logging tool can't provide enough information for best-detecting

lithology, but the combination of data from more than one logging tool is definitely very helpful in determining the lithology of the logged section (Bateman, 1985).

The recorded Neutron and Density data were used to determine the common lithology of the studied unit in well BB-1 (Figure 4). It's very clear that Unit A of the Kurra Chine Formation consists of anhydrite, anhydritic dolostone, and dolostone as the main lithology with an obvious ratio of dolomitic limestone and limestone. The scattering of sample points towards the gas region or towards the shale region is not so obvious.

Accordingly, neither high shale content is expected to exist in the studied Unit A of the Kurra Chine Formation, nor a high ratio of gas saturation within the pore spaces of the unit.

The plotted M-N crossplot for the studied Unit A of the Kurra Chine Formation from the three selected wells is shown in Figure 5. Domination of dolostone and anhydrite was also approved by the M-N crossplot with an obvious percentage of dolomitic limestone and limestone content in the unit.

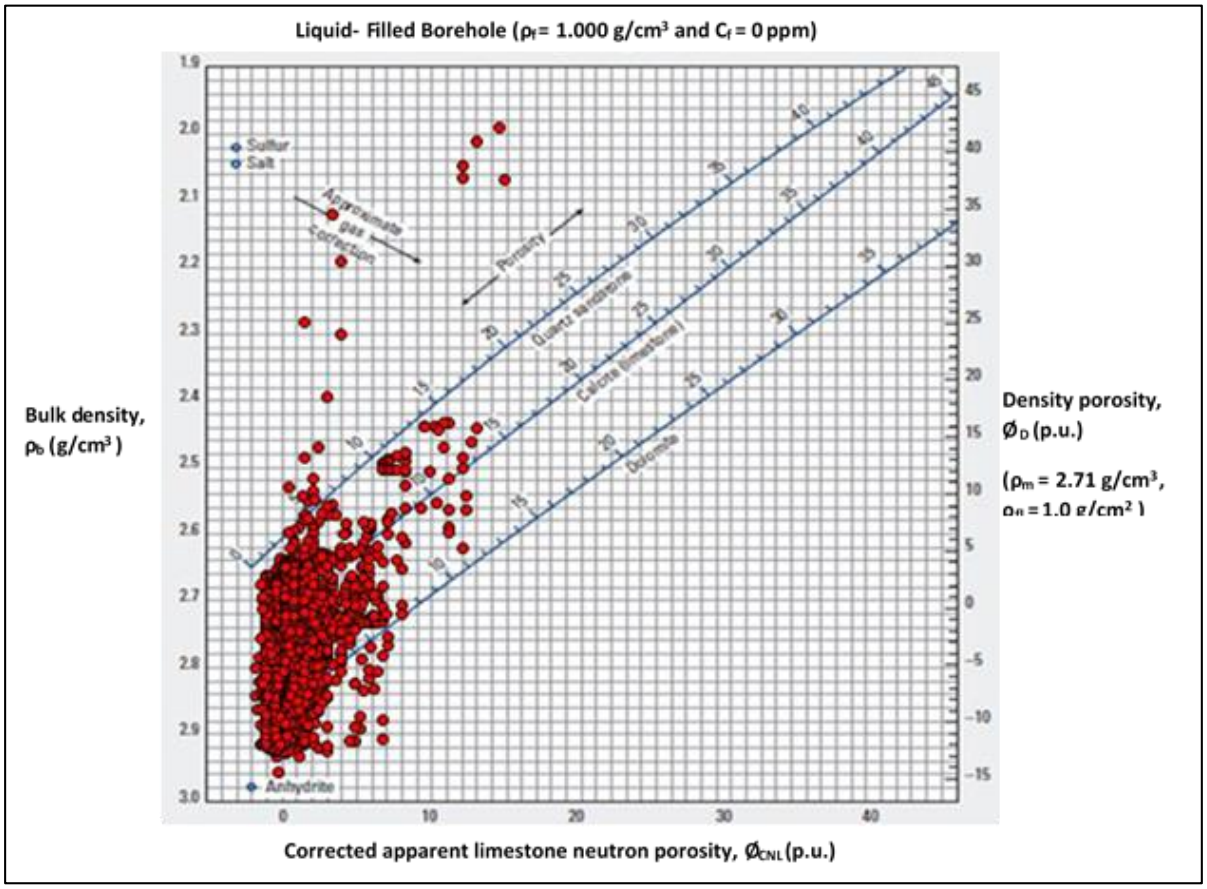

Figure 4. The neutron-density crossplot shows the lithology identification of Kurra Chine's Unit A in the well BB-4.

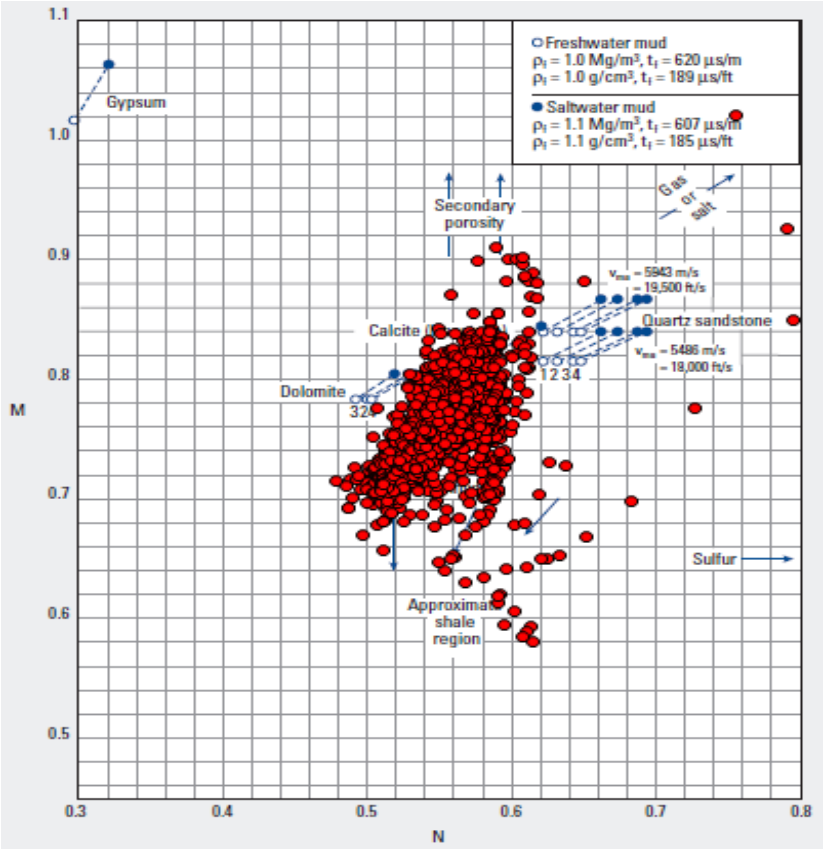

Figure 5. M-N cross plot for determining lithology of the Kurra Chine A Unit in the well BB-4.

6. Gamma Ray Log and Shale Content

Even though the Gamma Ray Log is a crucial part of the conventional investigation of shaly formations, it might be difficult to understand this measurement (Ellis & Singer, 2007).

The record of the Gamma-ray logs for the studied Unit A of the Kurra Chine Formation in the BB-4 well is shown in Figure 6A.

The well BB-4 showed a relative increase in the Gamma-ray record at the middle and lower parts of the studied Unit A of the Kurra Chine Formation. The highest deflection of the Gamma-ray curve exists at the lowermost part of the studied unit which gradually decreases toward the middle and upper parts of the unit. A slight increase in the Gamma-ray record near the top of the studied unit is noticeable.

The process of formation evaluation in terms of reservoir characterization has long been difficult without estimating shale volume. Clay minerals and shale are affected by all well-logging tool readings by a few degrees. At the moment of illustrating porosity and water saturation as reservoir parameters, the affected shale content has to be measured (Bassiouni, 2008).

There could be a linear or non-linear relationship between shale content and gamma-ray magnitude. All of the relationships are empirical (Krygowsky, 2003).

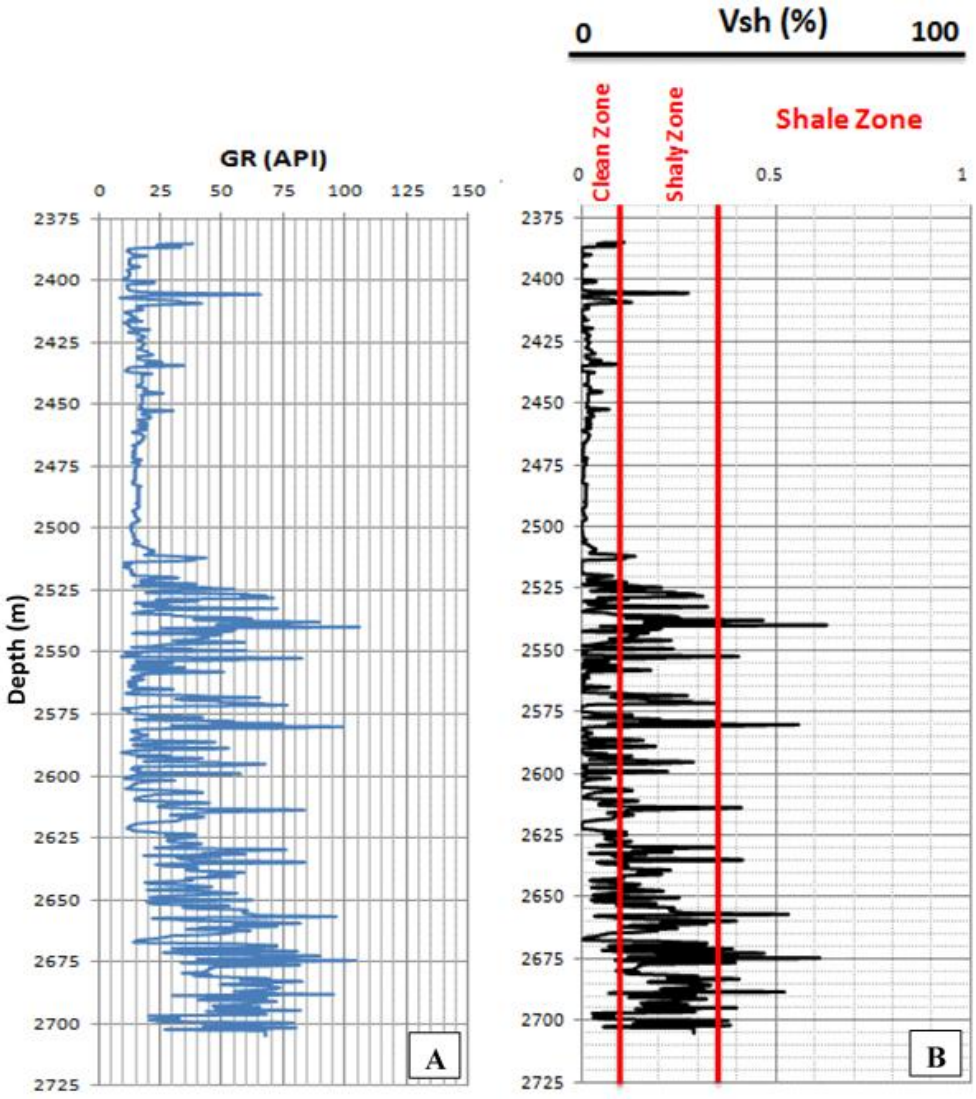

Figure 6. A) Gamma-ray log record and B) the calculated shale content for Unit A of the Kura China Formation in BB-4 well.

For Unit A of the Kurra Chine Formation under study, the shale volume was calculated from the Gamma-ray logs by first calculating the Gamma-ray index (GRI) (Eq. 1) and then using the formula proposed by Larionov (1969) for shale volume calculation in consolidated rocks older than Tertiary (Eq. 2). Figure 6B shows the calculated shale volume of Unit A of the Kurra Chine Formation.

$$GRI = \frac{\mathrm{GRlog} - \mathrm{GRmin}}{GRmax - GRmin} \quad (1)$$

$$Vsh = 0.33[2^{(2*GRI)} - 1.0] \quad (2)$$

Where: GRI: Gamma-ray index; GRlog: Recorded gamma-ray at any depth; GRmin: Minimum recorded gamma ray (clean zone); GRmax: Maximum recorded gamma ray reading (shale zone); Vsh: Shale volume.

Narrow shale beds (shale content >35%) at different depth intervals exist in the lower and middle parts of the studied unit in the BB-4 well. Additionally, a lot of shaly intervals (shale content between 10 and 35%) of variable thicknesses also co-existed at the lower and middle parts of the studied unit, especially in the lowermost part which intercalated by clean intervals of less than 10% shale content (Ghorab et al., 2008). The upper part of the studied Unit A of the Kurra Chine Formation in the well BB-4 is generally clean.

7. Porosity and Permeability

The porosity determination logging tools have responses to the rock matrix and fluid filling the pore voids. Therefore, the measuring porosity tools reflect the rock types, the clay content, and the fluid types with an indication of porosity (Bateman, 1985).

Conventional porosity logs (Sonic, Density, and Neutron) are one of the main tools that assist in providing continuous information about the porosity of the reservoir beds along the logged section of the well.

In this study, data from Sonic, Density, and Neutron logs are used to calculate, as precisely as possible, the porosity of the studied Unit A of the Kurra Chine Formation in BB-4 well.

Shale and clay, as soft materials, are increasing the recorded Δt by the Sonic logging tool. Thus, the calculated ØS using equation 3 will be higher than the true value of the porosity in a ratio proportional to the shale volume. The same is true when ØD is calculated through the recorded ρb values. The low density of shales and clay relating to the other rock matrix causes mistakenly calculation of ØD when Equation 4 is applied.

$$ØS = \frac{\Delta tlog - \Delta tmat}{\Delta tfl - \Delta tmat} \quad (3)$$

Where: ØS = Sonic porosity (fraction); Δtlog: Interval transit time in the formation (μsec/ft); Δtfl= Fluid travel time (μsec/ft); Δtma= Interval transit time of formation's matrix (μsec/ft).

$$ØD = \frac{\rho mat - \rho b}{\rho mat - \rho fl} \quad (4)$$

Where: ØD: Density porosity (fraction); ρmat: Density of the matrix (gm/cc); ρb: Bulk density at any depth (gm/cc); ρfl: Density of the mud filtrate (gm/cc).

The shales and clays have to be issued to illustrate neutron porosity also for the reason that the hydroxyls are linked with the structure of the clay mineral. The great obvious porosity ratios are due essentially to the hydrogen concentration associated with the shale matrix (Ellis & Singer, 2007).

Therefore, using the recommended formulas by Dewan (1983), namely equations 5, 6, and 7, the calculated porosity values from shale impact are corrected for the three porosities of ØS, ØD, and ØN (Figure 7).

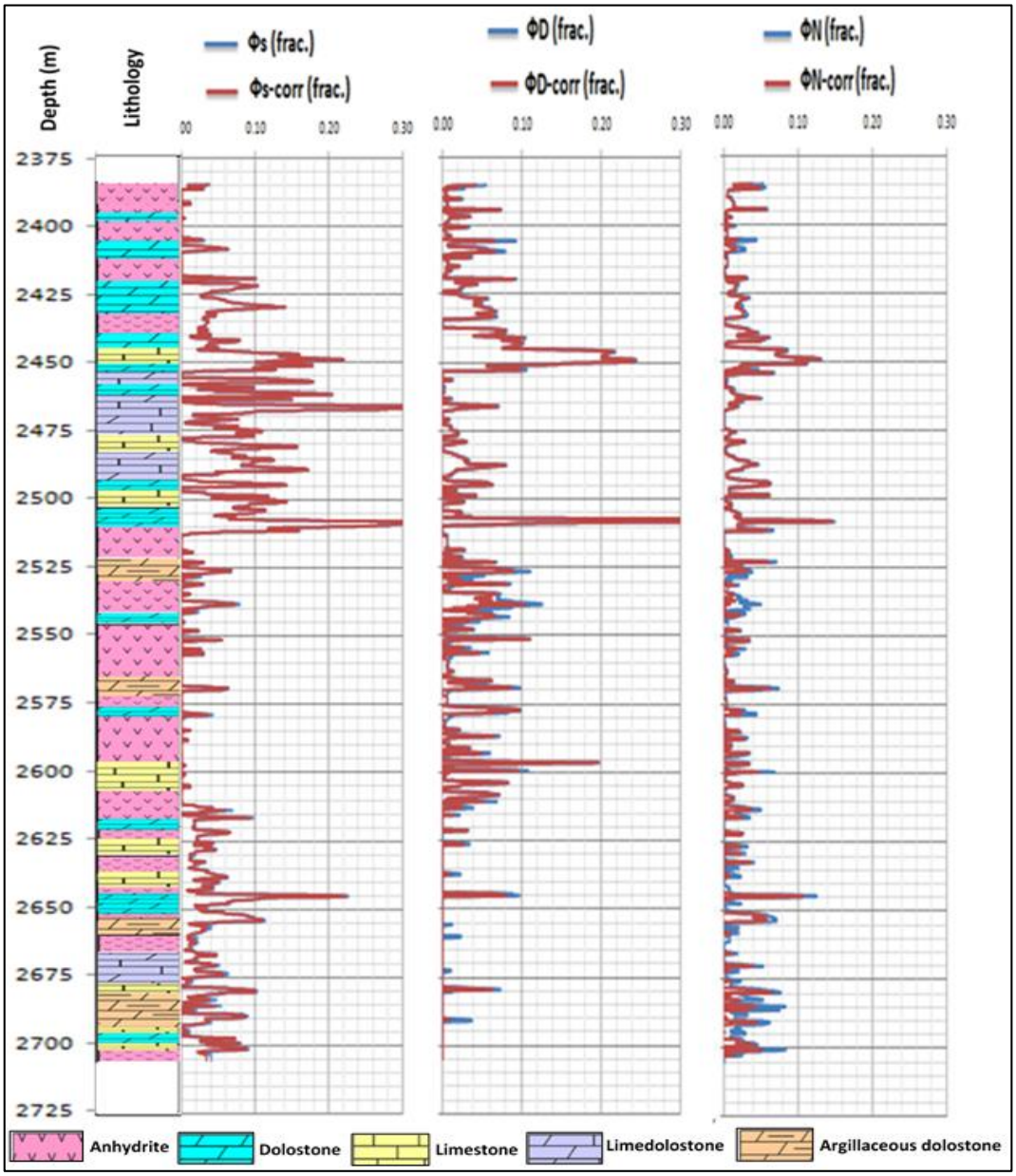

Figure 7. Incorrected and corrected Sonic, Density, and Neutron porosities from shale effect for Unit A of the Kurra Chine Formation in well BB-4 along with the common lithology of the unit.

$$\emptyset Scorr = \emptyset S - (Vsh * \emptyset Ssh) \quad (5)$$

Where: ØScorr: Corrected sonic porosity from shale effect; ØS: Calculated porosity from sonic log data (without correction); Vsh: Shale volume; ØSsh: Sonic porosity for adjacent shale.

$$\emptyset Dcorr = \emptyset D - (Vsh * \emptyset Dsh) \quad (6)$$

Where: ØDcorr: Density corrected porosity from shale impact; ØD: Density porosity (incorrect); ØDsh: Density porosity for adjacent shale; Vsh: Volume of shale.

$$\emptyset Ncorr = \emptyset N - (Vsh * \emptyset Nsh) \quad (7)$$

Where: ØNcorr: Corrected neutron porosity from shale effect; ØN: Recorded incorrect neutron porosity; ØNsh: Neutron porosity for adjacent shale; Vsh: Shale volume.

The distribution mechanism of the shale content inside the pore spaces and around the rock grains can be ascertained with the use of the values of ØD and ØN. Based on the proposed crossplot by Thomas & Stieber (1975) for determining shale distribution mode in sandstone reservoirs and its applications in carbonate reservoirs (Yang, 2015; Moradi et al., 2016; Baban & Ahmed, 2022; Baban et al., 2020) in the investigated Unit A of the Kurra Chine Formation in the researched BB-4 well, dispersed type proved to be the predominant style of shale distribution (Figure 8).

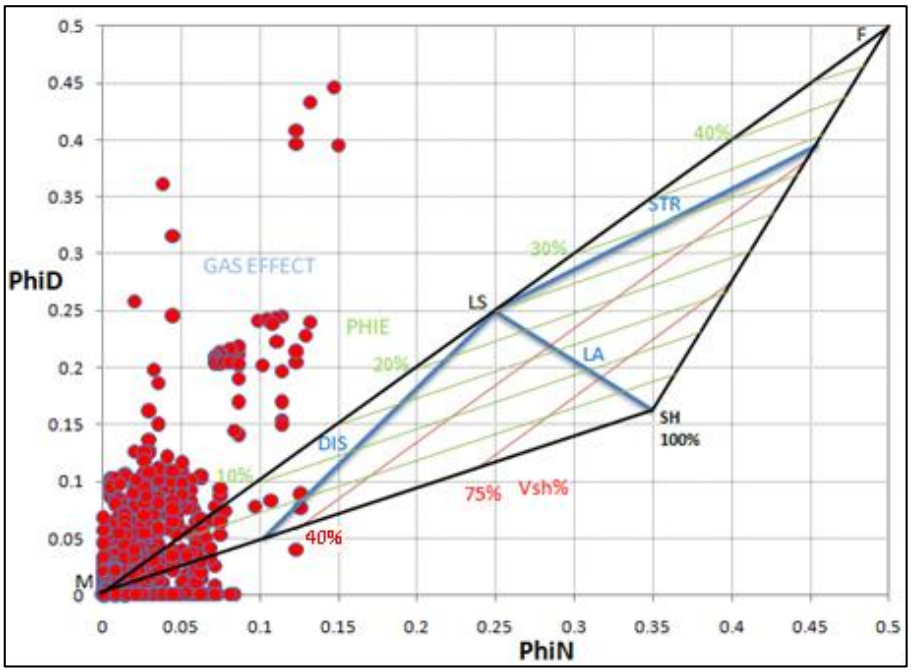

Figure 8. Thomas-Stieber crossplot for Unit A of the Kurra Chine Formation in well BB-4 to show the shale distribution styles (structural, laminated, and dispersed).

Determining the values of ØD and ØN for the nearby shale bed (the point of SH100% on the crossplot) and taking M-SH100% as the zero porosity line aids in correcting the porosity caused by the shale effect. Thus, the corrected porosity estimates for the unit under study primarily

showed a decrease in porosity of less than 7%, depending on the rate of shale content. Scattering of the sample points upwards in the crossplot indicates a possible gas effect.

The average values of the ØDcorr and ØNcorr, which are known as combination ØNDcorr, are generally dependent when evaluating reservoir rocks' porosity. The calculated ØNDcorr values represent the total porosity of the rock that is corrected from shale impact and even gas impact.

Figure 9A shows the calculated ØND and ØNDcorr for the studied Unit A of the Kurra China Formation in BB-4 well which looks like most parts of the unit have less than 5% porosity with exceptionally greater than 10% porosity in only 4 narrow horizons.

The secondary porosity (fractures, voids, vugs, …etc) for the studied unit (ØSec) has been calculated by applying the conventional method of subtracting the corrected sonic porosity (ØScorr) value from the calculated neutron–density combination corrected porosity (ØNDcorr) (Figure 9B). The calculated ØSec values ranged generally between 0 and less than 8% and the exceptionally high secondary porosity at depth interval 2551 – 2552 m is definitely not related to fractures.

The detected secondary porosities are concentrated at the upper and near the middle part of the studied Unit A where the ØNDcorr showed relatively higher values compared to the other parts of the unit.

Predicting the existence of permeable intervals can be done for any reservoir depending on some kinds of logs, such as Caliper and Spontaneous Potential (SP), but without measurement unit values (millidarcy). The exception is the Nuclear Magnetic Resonance (NMR) log, by which permeability is recorded directly as values in millidarcy.

For some data categories, including permeability or rock textural metrics, core samples are the most reliable source. A real Darcy permeability is the one that was measured in the laboratory. In the wellbore, there is more than one fluid phase competing for pore space. The result is that the permeability estimated is an “effective permeability” (the permeability of one fluid phase at less than 100% saturation of that phase (Bowen, 2003).

In this study, the data of permeability for the whole of Unit A of Kurra Chine Formation was available for the well BB-4 (Figure 10). The permeability recorded by the NMR log for the studied unit in this well is directly used in the evaluation process.

Zones of poor to fair permeability (1 – 15 mD) according to North (1985) can only be seen in a few depth intervals, mainly at the upper part of the unit between depths 2443 m and 2447 m, whereas moderate to good permeability is observed only between depths 2447 m and 2448.4 m, where permeabilities between 20 mD and 65.5 mD are recorded. Most parts of the unit are of very poor permeability (less than 1.0 mD) which sometimes extends to tens of meters thicknesses, primly at the lower portion of the formation.

It is important to mention that the zones identified to have secondary porosities (Figure 9B), showed no noticeable permeabilities especially the zone between depths 2515 and 2610 m. Accordingly, and as concluded previously, the calculated secondary porosities are more likely to be from moldic porosities, voids, or vugs rather than from fractures.

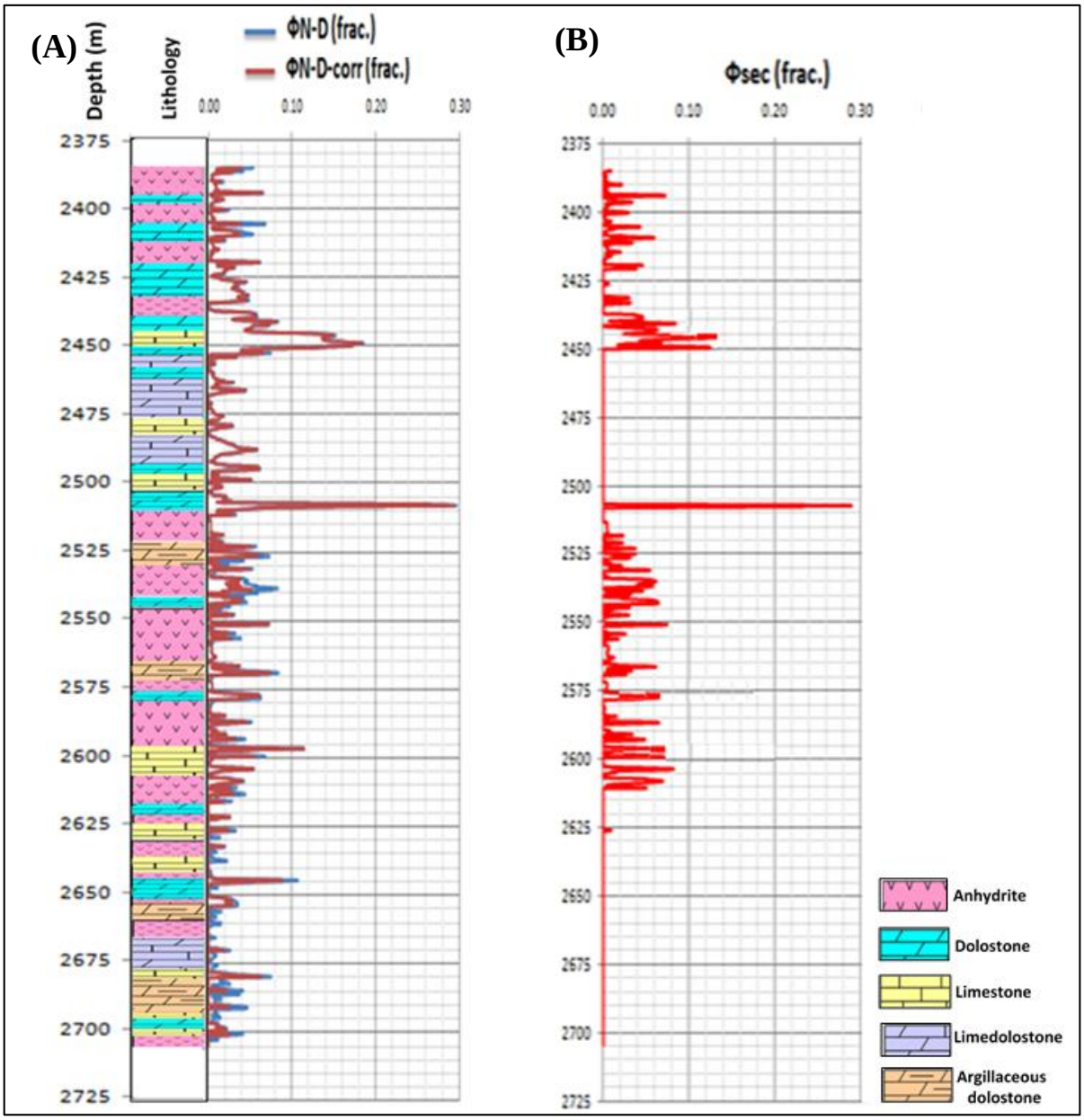

Figure 9. A) AIncorrected (ØND) and corrected combination Neutron-Density porosity (ØNDcorr) from shale effect for the Unit A of the Kurra Chine Formation in well BB-4. B) Secondary porosity (Øsec) plot for the studied A Unit of the Kura China Formation in well BB-4.

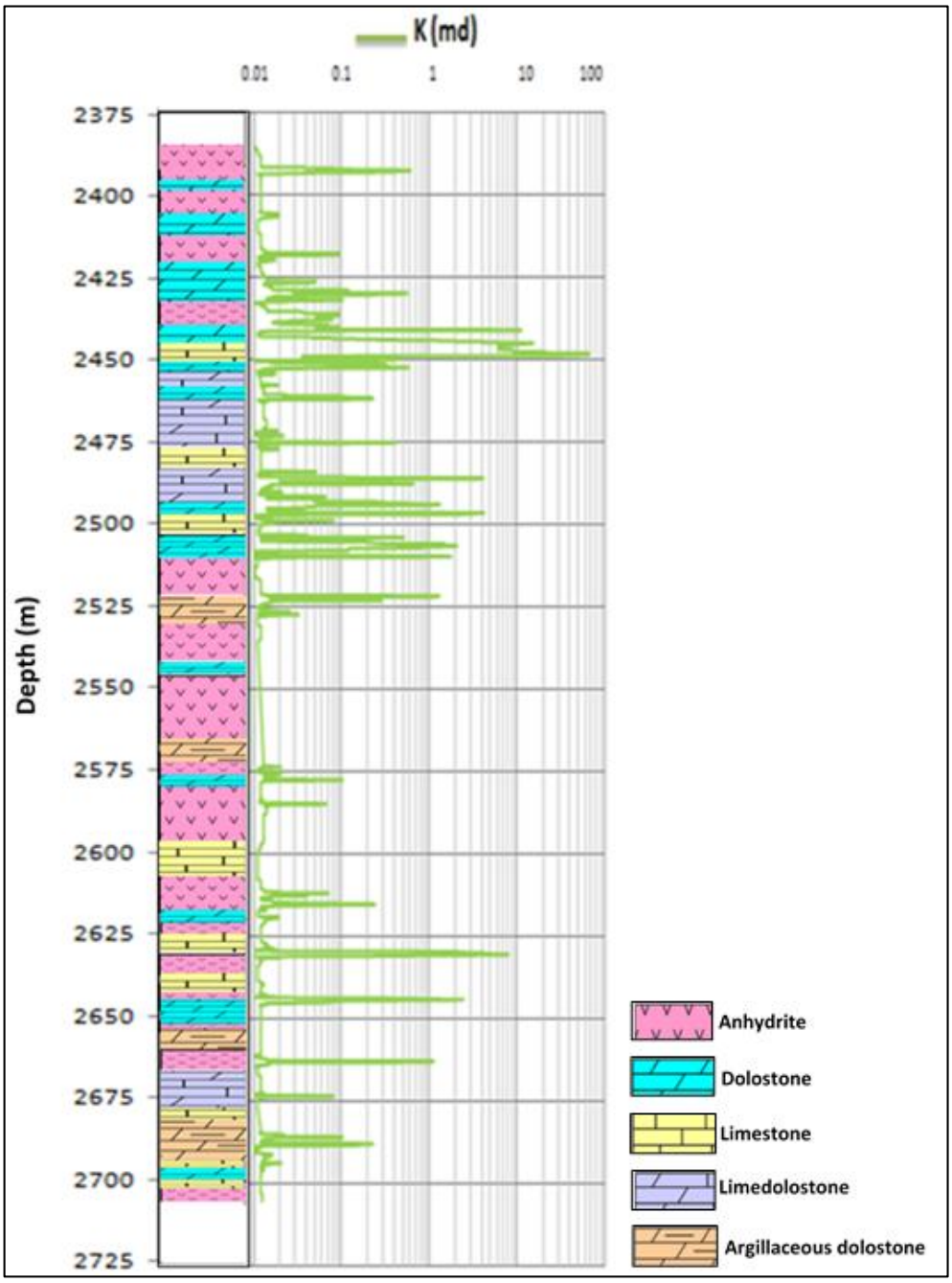

a

Figure 10. The plot of the recorded permeability from the NMR log for the studied Unit A of the Kurra China Formation in well BB-4.

8. Reservoir Units

In order to show the reservoir properties of the studied Unit A of Kurra Chine Formation as precisely as possible, the unit in well BB-4 has been subdivided into a number of distinguished reservoir units (RU) based on variations in shale content, porosity, and permeability.

Figure 12 shows the identified reservoir units of Unit A of the Kura Chine Formation in the studied well BB-4 and Table 1 summarizes the minimum, maximum, and average values of the

mentioned three parameters of shale content, porosity, and permeability. The table also shows the depth interval of each reservoir unit within the studied well.

In well BB-4, the RU-1 is located at the depth interval between 2385 and 2525 m (Figure 11). The average shale content of this reservoir unit is about 14% with an average porosity of about 3% (poor porosity according to North (1985) (Table 1). RU-1 is generally of negligible to poor permeability (about 0.69 mD as an average permeability). The dominant lithology of the RU-1 in the well BB-4 is anhydrite, dolostone, limedolostone, and limestone.

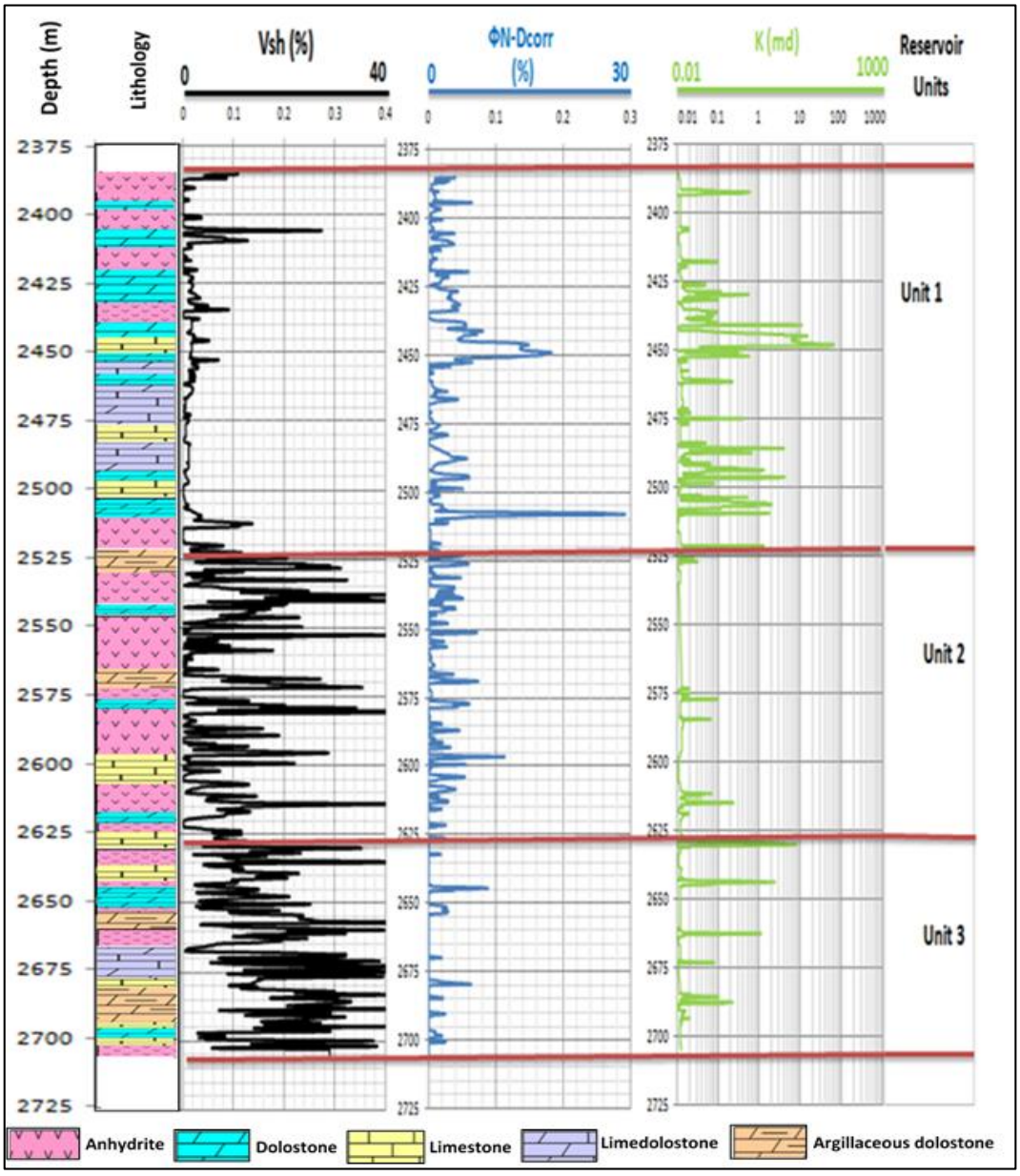

Figure 11. Subdivision of the studied Unit A of the Kurra Chine to reservoir units based on the shale volume, porosity, and permeability for well BB-4.

Table 1. The lowest, highest, and average shale content values, with porosity and permeability for the notable reservoir units of Unit A of the Kurra Chine Formation in well BB-4.

	Depth Interval (m)	Statistics	Vsh (%)	Porosity (%)	Permeability (MD)	Main Lithology
RU- 1	2385-2525	Min	1.00	0.5	0.007	anhydrite, dolostone, limedolostone, and limestone.
		Max	27.80	6.5	65.5	
		Average	14.4	3	0.69	
RU-2	2525-2625	Min	2.5	1.2	0.001	anhydrite, dolostone, argillaceous dolostone, and limestone
		Max	40	11.8	0.24	
		Average	21.25	6.5	0.014	
RU-3	2625-2705	Min	14.8	2	0.009	limestone with interbedded anhydrite, limedolostone, and argillaceous dolostone
		Max	40	8.5	8.0	
		Average	27.4	5.25	0.09	

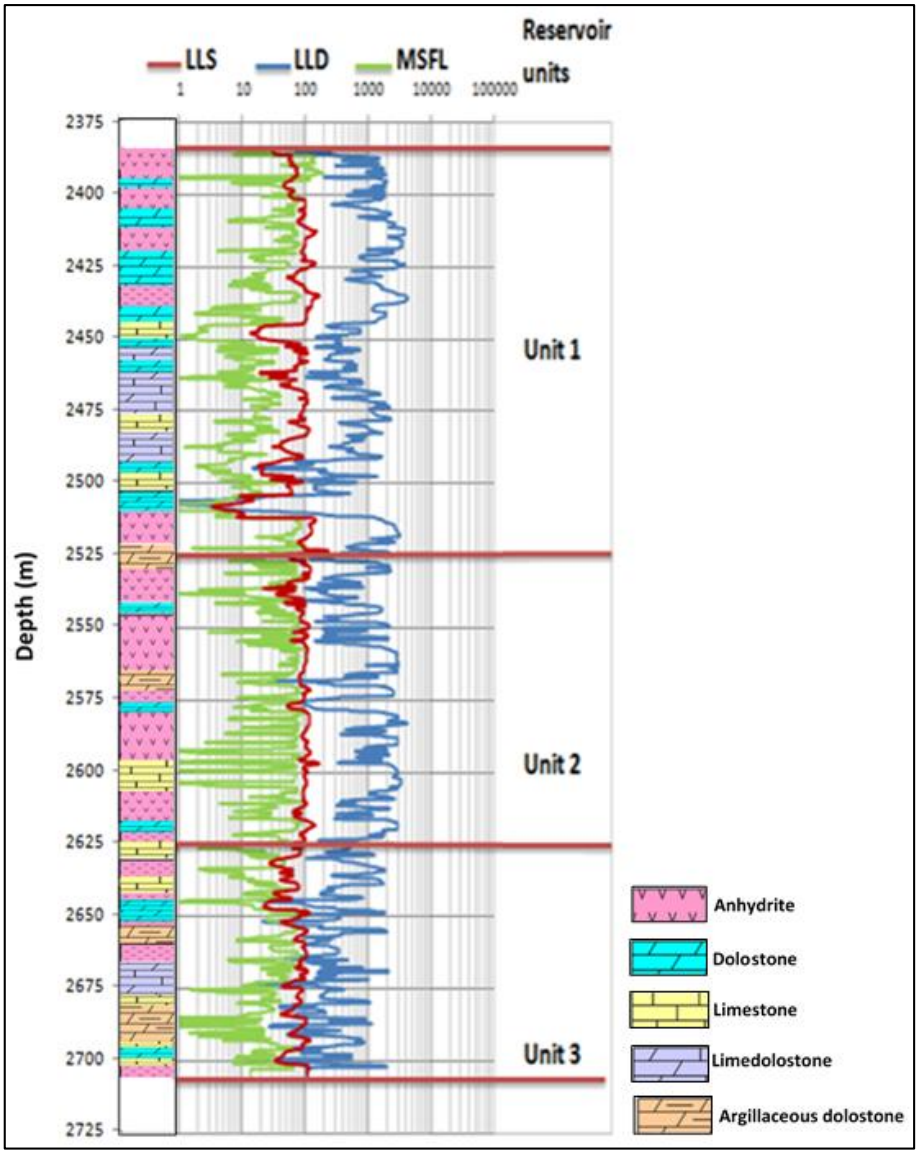

Figure 12. Rxo (MSFL), Ri (LLS), and Rt (LLD) curves for the studied Unit A of the Kura China Formation in well BB-4.

RU-2 is located between depths 2525 and 2625 m and is characterized by relatively high shale content (> 21% as an average) with the existence of a number of horizons of higher than 35% shale content. The average porosity of RU-2 in the BB-4 well is about 6.5% (poor porosity) and its permeability is almost negligible (about 0.14 mD as average permeability). The dominant lithology of RU-2 is anhydrite, dolostone, argillaceous dolostone, and limestone.

RU-3 reservoir unit is observed between depths 2625 m and the base of the studied Unit A at depth 2705 m. RU-3 is composed mainly of limestone with interbedded anhydrite and limedolostone in addition to argillaceous dolostone.

This unit contains the highest average shale volume (about 27%) among the distinguished reservoir units in this study. The porosity is considered to be poor (average 5.25%) with no record of any horizons having porosity greater than 8.5%. The permeability of RU-3 in the well BB-4 is also negligible to poor (average 0.09 mD) where a lot of non-permeable horizons are intercalated with poorly permeable intervals indicating a non-homogeneous lithology of this reservoir unit.

9. Hydrocarbon Saturation

The resistivity log data for Unit A of the Kurra Chine Formation in the selected well BB-4 are used to estimate the hydrocarbon saturation in each of the identified reservoir units.

The available resistivity logs for this study included Microspherically Focused Log (MSFL), Shallow Laterolog (LLS), and Deep Laterolog (LLD) which their recorded values considered resistivity of the flushed zone (Rxo), the resistivity of the transition zone (Ri), and resistivity of the uninvaded zone (Rt, true resistivity), respectively (Figure 12).

The separation pattern between the three resistivity curves mostly provides information about the fluid types within the reservoir void spaces (considering the type of drilling mud).

Since the well under study was drilled using saline water-based mud, it is anticipated that the three resistivity type curves will clearly separate in hydrocarbon-bearing layers (being Rxo the lowest). The separation between the three resistivity curves should be more obvious in those intervals where porosity is relatively high. In the zones where the lithology is dense and/ or they are water-bearing zones; no separation between the three resistivity logs of Rxo, Ri, and Rt is expected to be observed.

From the pattern and values of the three resistivity logs, hydrocarbon-bearing horizons are expected to exist in the studied Unit A in well BB-4 especially at the upper and middle parts of the formation (RU-1 and RU-2).

Archie equation (Eq.8) is the most popular equation used for calculating water saturation from log data.

$$Sw = (F * \frac{Rw}{Rt})^{1/n} \quad (8)$$

Where: Sw: Water saturation in the uninvaded zone (in fraction); F: Formation resistivity factor; Rw: Formation water resistivity (in ohm.m); Rt: True resistivity (in ohm.m); n: Saturation exponent (its value ranges from 1.8 to 2.5 but mostly 2.0 is applied).

Formation resistivity factor (F) as suggested by Archie (1942 in Asquith & Gibosn, 1982) can be related to porosity by Equation 9:

$$F = a/\emptyset^m \quad (9)$$

Where: F: Formation resistivity factor; a: Tortuosity factor (complexity of the paths and is equal to the value 1.0 for carbonates, the case of this study); Ø: Porosity; m: Cementation factor.

On the other hand, water saturation in the flushed zone (Sxo) also similarly can be calculated using Equation 10 in which formation water resistivity (Rw) is replaced by mud filtrate resistivity (Rmf) and true resistivity (Rt) replaced by resistivity of the flushed zone (Rxo).

$$Sxo = (F * \frac{Rmf}{Rxo})^{1/n} \quad (10)$$

In this study, the value of Rw is obtained from the final report of the studied BB-4 well and was equal to 0.01 Ω.m.

The best methods for determining cementation exponent (m factor) are either through testing selected core samples in the laboratory or through Picket crossplot using the log-derived values of porosity, values of true resistivity, and considering the value of Rw when drawing a line passing across the sample points at the lower left side of the crossplot (100%Sw). In this study, the second-mentioned method is used as shown in Figure 13. The inverse slope of the mentioned line which represents the m value appeared to be equal to 1.55 for the Unit A of the Kurra Chine Formation in well BB-4.

As values for all of the requested factors for applying Archie equations (Eqs. 8 and 10) are available, it's time to calculate values of water saturation in the uninvaded zone (Sw) and the invaded (flushed) zone (Sxo). Additionally, both values of residual and movable hydrocarbon saturations also can be calculated using equations 11 and 12, respectively.

Figure 14 shows the calculated Sw, Shr, and Shm for the studied Unit A of Kurra Chine Formation in well BB-4 with respect to the calculated ØNDcorr.

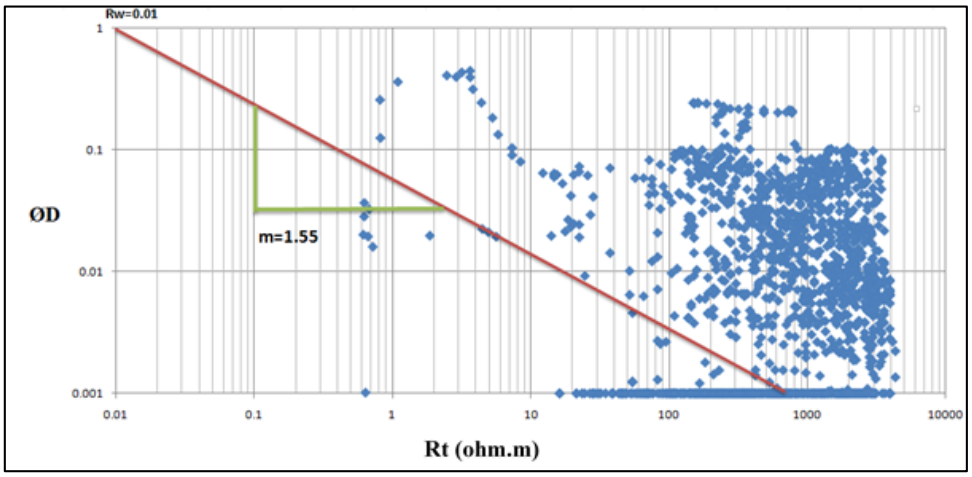

Figure 13. Determined cementation factor (m) value from Pickett crossplot for the studied Unit A of the Kurra Chine Formation in well BB-4.

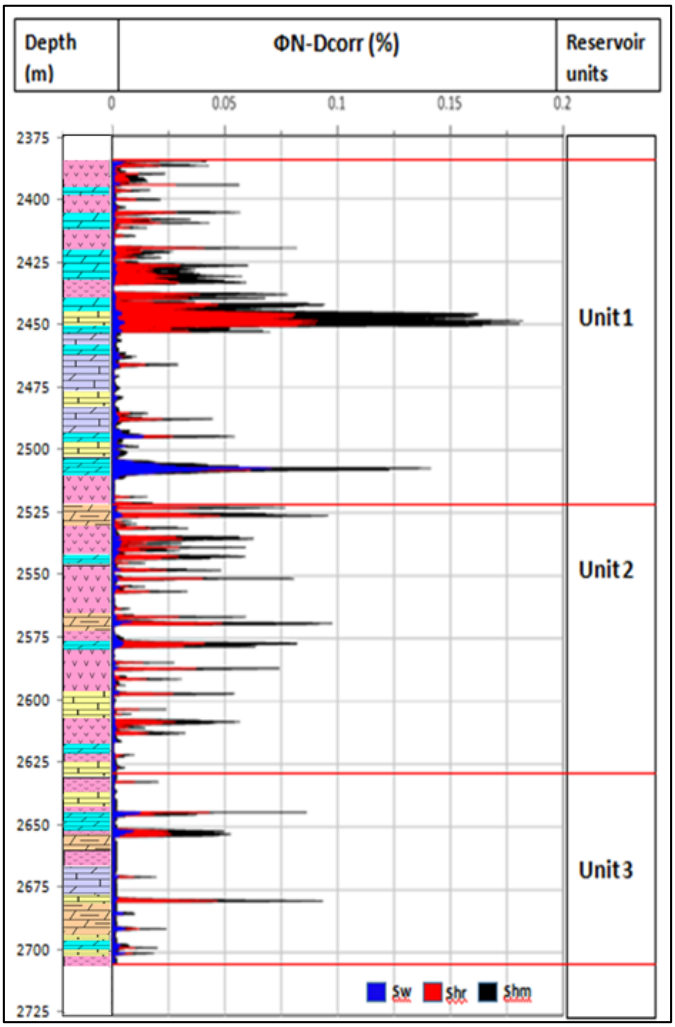

Figure 14. Distribution of water, moveable hydrocarbon saturations, and residual hydrocarbon saturations in well BB-4's pore spaces inside the Kurra Chine formation's Unit A under study.

$$Shr = 1 - Sxo \quad (11)$$

$$Shm = 1 - Sw - Shr \quad (12)$$

Where: Shr: Residual hydrocarbon saturation; Shm: Movable hydrocarbon saturation.

It is obvious that all of the distinguished reservoir units in the studied Unit A in well BB-4 contain hydrocarbons in different saturation ratios, and in all of the depth intervals, as porosity increases the hydrocarbon saturation also increases.

Generally, the highest percentage of hydrocarbons in the studied Unit A is of residual type. Although porosity of the Unit A in the well BB-4 is low (low hydrocarbon storage capacity), but observable percentage from the reservoired hydrocarbons is movable, especially in RU-1. A lot of water-bearing zones can also be seen separating the hydrocarbon-bearing zones in the well.

10. Hydrocarbon Movability and Flow Zone Indicator

There are different methods for detecting movable hydrocarbons in any reservoir. Well tests, such as the Drill Stem Test (DST) and Formation Test are very helpful in determining productive zones where movable hydrocarbons exist within the tested interval (Baker Hughes, 1992). On the other hand, well logging can provide necessary data for detecting movable hydrocarbon zones within a much wider depth interval.

One method for initially identifying zones of mobile hydrocarbons in any reservoir that depends on log data is the Movable Hydrocarbon Index (MHI).

The MHI is the ratio of the water saturation in the flushed zone (after invasion) to the water saturation at the un-invaded zone (Sw/Sxo) (Eq.13).

$$Sw/Sxo = [(\frac{Rxo}{Rt})/(\frac{Rmf}{Rw})^{1/n} \quad (13)$$

If the ratio of water saturation of the uninvaded zone to the water saturation of the flushed zone (Sw/Sxo) is equal to/ or greater than 1.0 there is no hydrocarbon moved or flushed out. If it is equal to / or less than 0.7 for sandstone and 0.6 for limestone, the hydrocarbon is moved (Asquith & Gibosn, 1982; Schlumberger, 1972, 1989; Asquith & Krygowski, 2004).

The movable Hydrocarbon Index of the reservoir units has been detected for Unit A of Kura China Formation in the studied BB-4well using 0.6 MHI cutoff (carbonate case) for differentiating movable from non-movable hydrocarbon bearing zones (Figure 15).

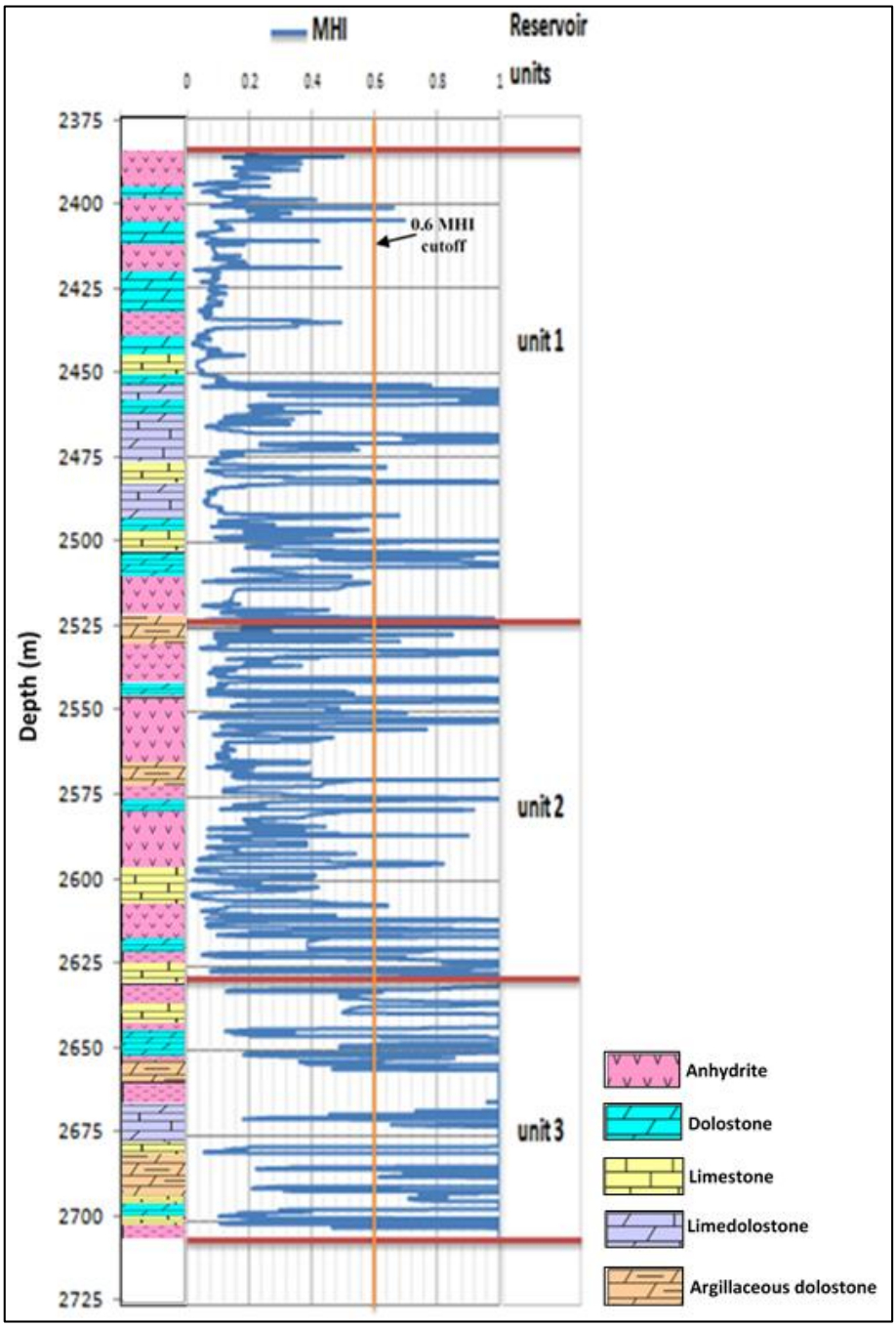

Figure 15. Movable Hydrocarbon Index for the studied Unit A of the Kurra Chine Formation in well BB-4 using 0.6 MHI as cutoff.

Regardless of the capacity of flow, there are a lot of movable hydrocarbon-bearing zones in Unit A especially in the reservoir units RU-1 and RU-2, whereas RU-3 contains a relatively lower number of productive horizons.

To show the flow efficiency in the studied Unit A of the Kurra Chine Formation based on the measured parameters from the available log data, the Flow Zone Indicator (FZI) proposed by Amaefule et al. (1993) is applied. Mean hydraulic radius and a modified Kozeny-Carmen

equation serve as the foundation for the original proposal of FZI. Since FZI is a unique parameter for every hydraulic flow unit, the FZI value varies for every type of reservoir.

The Hydraulic Flow Unit (HFU), on the other hand, is a continuous construction that covers a specified reservoir volume. Its nearly constant fluid and petrophysical characteristics define its unique static and dynamic communication with the wellbore (Tiab, 2000).

The values of FZI for any section are mostly based on the calculated Reservoir Quality Index (RQI) and the Normalized Porosity Index (Øz) both of them can be achieved from the productive porosity and permeability of the section as seen in equations 14 – 16.

$$RQI = 0.0314\ (\frac{K}{\emptyset e})^{1/2} \tag{14}$$

$$\emptyset z = \frac{\emptyset \mathrm{e}}{1 - \emptyset \mathrm{e}} \tag{15}$$

$$\mathrm{FZI} = \mathrm{RQI}/\ \emptyset \mathrm{z} \tag{16}$$

Where: FZI = Flow Zone Indicator in μm; RQI = Reservoir Quality Index; Øz= Normalized Porosity Index (pore volume to matrix volume ratio); Øe= Effective porosity in fraction; K = permeability in mD.

FZI values for the studied Unit A of the Kurra Chine Formation in BB-4 well have been calculated and shown in two different ways. The actual frequency (distribution) of the calculated FZI values (which are generally known as S-shape curves) is plotted as shown in Figure 16, and depending on the variations in the slopes of the curves, different ranges of FZI values are distinguished. On the other hand, the sample points in the RQI versus Øz crossplot (Figure 17) represent the FZI values from which a number of groups with different ranges of FZI values are also distinguished.

Six unique HFUs exist as flow systems, according to the computed FZI for Unit A of the Kurra Chine Formation in well BB-4. The identified HFU units, ranges, and average of the FZI values for each of the six identified HFU are listed in Table 2.

HU-2 flow type with average FZI values of about 4.53 looks to be the most dominant in Unit A of this well. The other dominant flow type in this well is RU-4 with a frequency of appearance of about 30% and an average FZI value of about 107.5.

Depending on the standard suggested by Fea et al. (2022) for describing the potentiality of the reservoir units, which is the average of the RQI and FZI values, most parts of Unit A of the Kurra Chine Formation in well BB-4 are either poor or tight reservoir quality (Table 2). On the

other hand, zones of excellent reservoir quality also exist in the unit, but they are less frequent and exist at different horizons in the three identified reservoir units.

Generally, with the highest degree of heterogeneity in any reservoir, a greater number of HFU units is expected. It should be noted that the hydraulic flow unit of the highest FZI value is considered the best in terms of permeability and flow capacity. Accordingly, HU-6 of the studied Unit A is most efficient for production if it occurs in zones of high percentages of hydrocarbon saturation, otherwise, the zone will produce water efficiently.

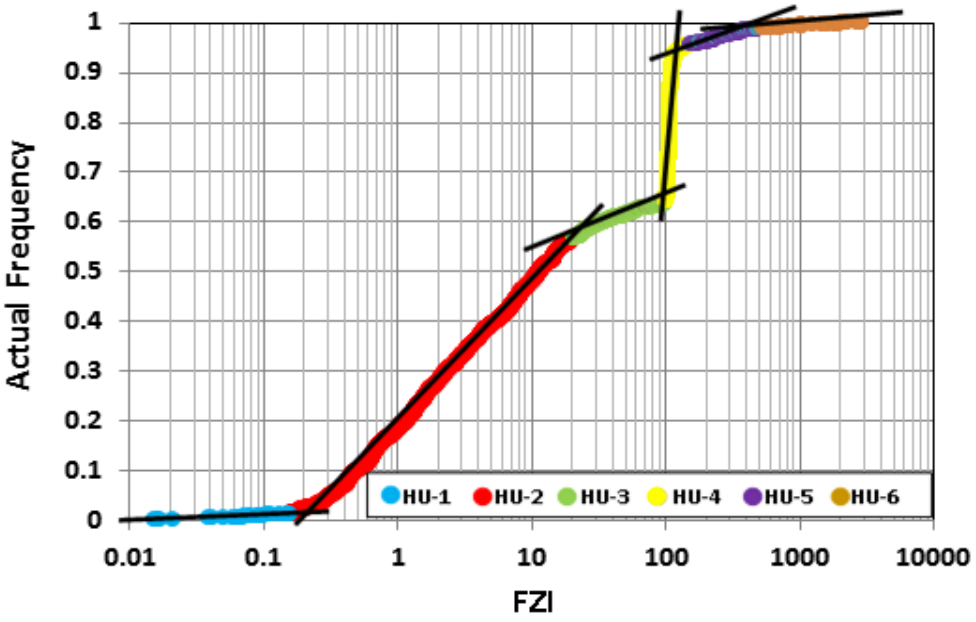

Figure 16. Real Frequency (distribution) of the computed Flow Zone Indicators (FZI) with the defined Hydraulic Flow Units (HFU) for Unit A of the Kurra Chine Formation under study in well BB-4.

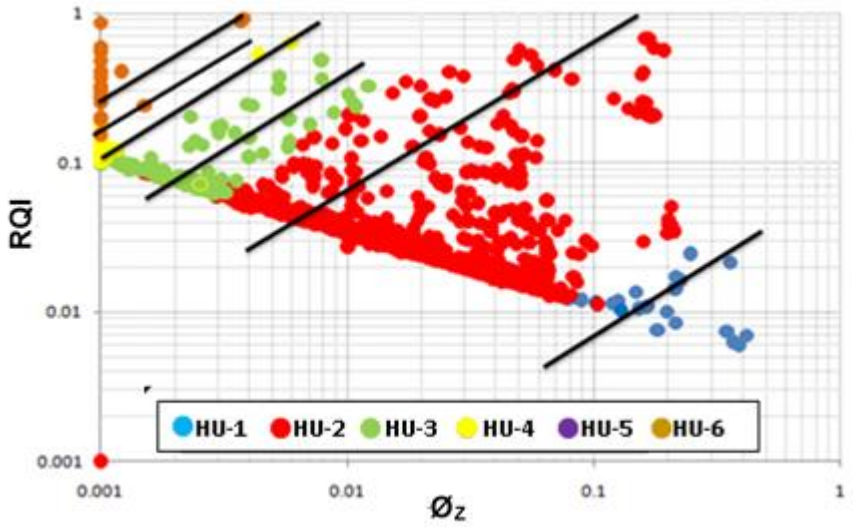

Figure 17. RQI versus Øz plots for Unit A of the Kurra Chine Formation in well BB-4 showing the clustered FZI values.

Table 2. The ranges and averages of the calculated FZI values and description of reservoir potentiality according to Fea et al. (2022) for each of the identified hydraulic flow units in Unit A of the Kurra Chine Formation in well BB-4.

Well	FZI Range	FZI Average	Hydraulic Units	Description of the reservoir potentiality
BB-4	0.015 – 0.16	0.079	HU-1	Tight
	0.16 – 21.07	4.53	HU-2	Poor
	21.07 – 101.118	47.56	HU-3	Excellent
	101.118 – 110.0	107.50	HU-4	Excellent
	110.0 – 154.227	117.80	HU-5	Excellent
	154.227 – 2969	623.49	HU-6	Excellent

11. Net to Gross reservoir and pay ratios

The productive (net) reservoir interval within the total (gross) reservoir intervals is defined as the net-to-gross or N/G ratio (Jahn et al., 2008). The differentiation between net and gross must be known in order to get the productive parts that contain a potential productive (net) reservoir of petroleum (Gluyas & Swarbrick, 2004).

To determine the reservoir's productive zones for hydrocarbon extraction, the terms "Cut-offs" and "Net to Gross" (NTG) are essential. The geologist may be concerned about the expense of evaluating existing hydrocarbons and, finally, calculating reserves that can be produced profitably (Egbele et al., 2005)

According to Egbele et al. (2005), net reservoir thickness is the overall thickness of the reservoir component known as having reservoir-quality rock. The tight rock and shaly components inhibiting flow are filtered off by applying the Vsh, Φ, and K cutoffs.

Accordingly, the mentioned ratios of N/G reservoir, N/G pay, and N/G productive can be estimated using selected cutoff values for staleness, porosity, permeability, water saturation, and MHI.

In this study, 35% as a shale cutoff value is selected as it’s the percentage proposed by Ghorab et al. (2008) to differentiate shaly from shale intervals.

The permeability threshold of 1.0 mD was determined by Peters, (2001); Law et al. (2001); Tiab & Donaldson (2012); Darling (2005); and Parnell et al. (2010) to differentiate between zones with effective oil flow ability and zones with none or very poor oil flow capacity. They also agreed about being 0.1 mD minimum permeability enough for gas to be produced from reservoirs. In this study, the value of 1.0 mD is selected as a permeability cutoff to differentiate zones of fluid flow ability from non-flow fluid zones.

The value for porosity cutoff has been determined using a porosity versus permeability crossplot (Figure 18). Accordingly, 3.6% appeared to be enough to provide the minimum

requested permeability (1.0 mD) for fluid to flow in the studied Unit A of Kurra Chine Formation in well BB-4.

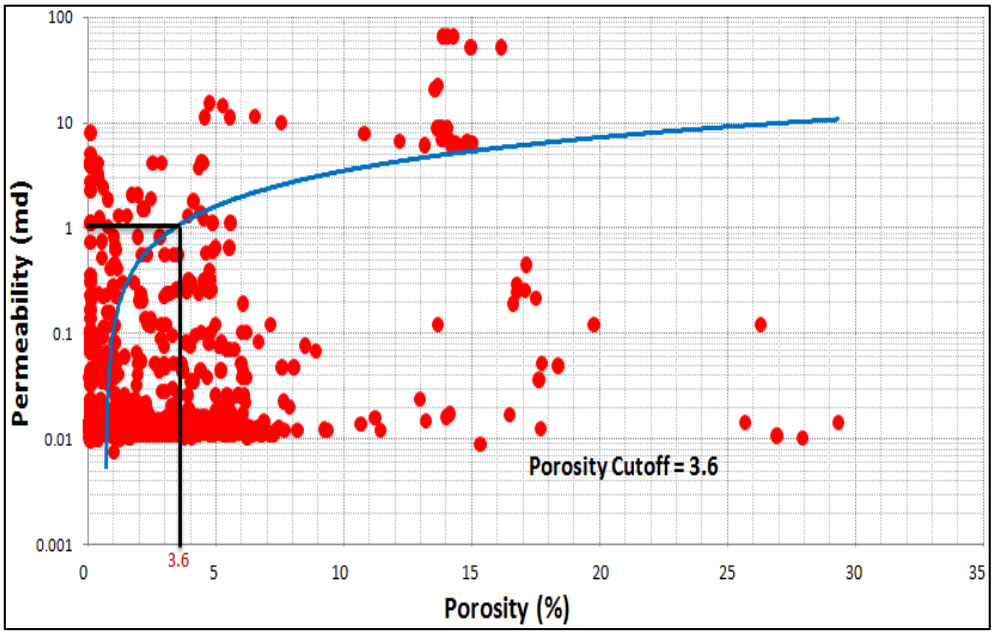

Figure 18. Porosity versus Permeability crossplot to establish a porosity cutoff value for well BB-4's Unit A of the Kurra Chine Formation.

In order to select the proper water saturation cutoff to differentiate pay intervals from non-pay intervals, the crossplot of porosity versus water saturation is used as shown in Figure 19. Thus, the maximum allowed value for Sw as a cutoff was 28%. As Unit A of Kurra Chine Formation is lithologically considered a carbonate unit, therefore, the previously mentioned MHI cutoff of 0.6 is selected in this study to distinguish between effectively productive from non-productive horizons and taking values of FZI values to differentiate the highly productive from less productive zones.

Table 3 shows the calculated N/G reservoir, pay, and productive ratios for the identified reservoir units of the studied Unit A of the Kurra Chine Formation in well BB-4.

The studied Unit A in well BB-4 looks to be generally of low reservoir properties as only about 9.2% N/G reservoir, 3.28% N/G pay, and 3.28 N/G productive ratios have been calculated which are equal to 34m net reservoir thickness and 15m net pay and productive thicknesses out of the 323m of the complete Unit A thickness. RU-2 in this well, with no net reservoir or pay thicknesses considers the worst among the three identified reservoir units.

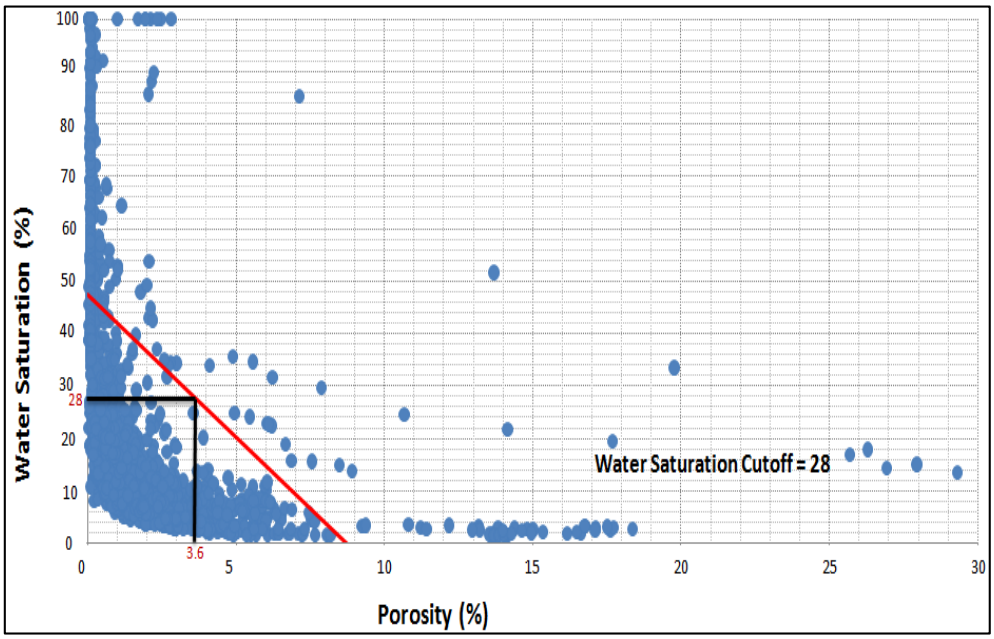

Figure 19. Water saturation versus porosity crossplot to establish a water saturation cutoff value for well BB-4's Unit A of the Kurra Chine Formation.

Table 3. Measured N/G reservoir, pay, and productive ratios for the reservoir units of the studied Unit A of the Kurra Chine Formation in well BB-4.

Reservoir units	Gross Thickness (m)	Net Reservoir Thickness (m)	Net pay Thickness (m)	Net Productive Thickness (m)	N/G Reservoir Ratio (%)	N/G Pay Ratio (%)	N/G Productive ratio (%)
RU-1	141	29	15	15	20.5	10.6	10.6
RU-2	101	0	0	0	0	0	0
RU-3	81	5	0	0	6.17	0	0
Total & Average	323	34	15	15	9.2	3.28	3.28

The depth intervals at which the net reservoir, pay, and productive intervals are identified from the studied Unit A of the Kurra Chine Formation in well BB-4 are shown in Figure 20.

It is important to mention that low porosity and permeability are the main causes of being Unit A of the Kurra Chine Formation in BB-4 well of such low productive capacity. Neither shale content, nor hydrocarbon saturations or movability represent problems for the unit. Accordingly, it can be concluded that the dominant anhydritic nature of the lithology with the expected compaction during the long periods of burial might cause such a reduction in the porosity and permeability of the unit. Additionally, the effects of the porosity-destructive diagenesis processes should not be out of expectation in such a carbonate nature reservoir unit.

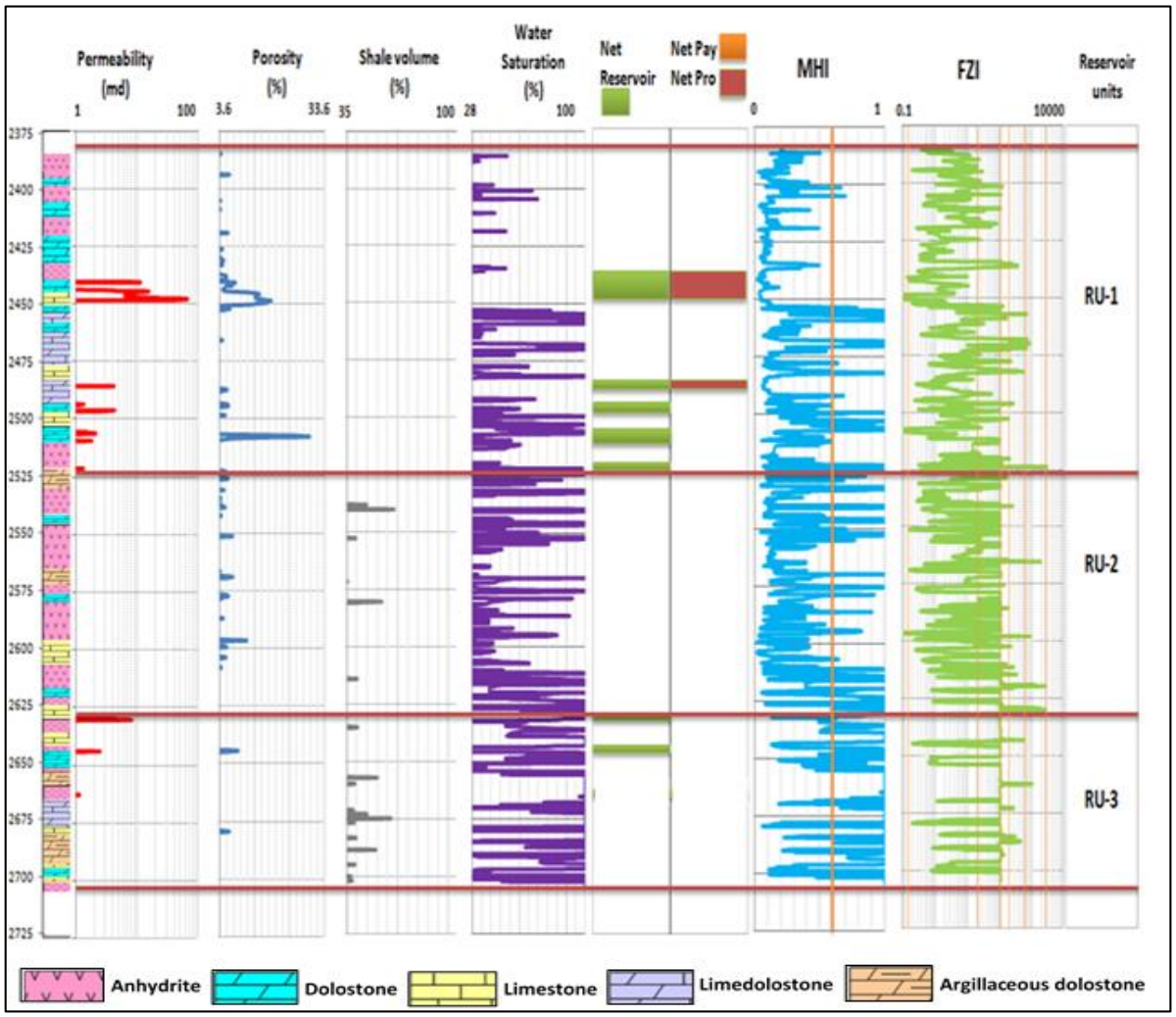

Figure 20. Location of the net reservoir and pay thicknesses using different cutoffs for the studied Unit A of the Kurra Chine Formation in well BB-4.

6. Conclusions

The most important conclusion that this study has come to about Unit A of the Kurra Chine Formation in well BB-4 can be summarized as that dolostone, anhydritic dolostone, and anhydrite are the common lithologies of the unit, along with dolomitic limestone and limestone. A lot of shaley intervals of variable thicknesses also co-exist at the lower and middle parts of the studied unit in well BB-4, especially in the lowermost part of the unit, which is intercalated by clean intervals of less than 10% shale content. In addition, the existing shale in the studied Unit A is in a dispersed mode of distribution, so it causes an effective reduction in the porosity and permeability of the unit. The unit is generally of poor porosity, with less than 10% in most parts and even negligible porosity, with less than 5% in a lot of its zones. The secondary porosities are obviously contributing to the total porosity of the unit, which is generally of poor permeability. Depending on the differences in the shale volume, porosity, and permeability values, Unit A under study can be split into three reservoir units. RU-1 has the best reservoir properties among the three. Unit A in well BB-4 is generally of low reservoir properties,

especially in the RU-2 and RU-3 reservoir units, where the common anhydritic lithology and the relatively high shale content both affect the porosity and permeability of the unit. Moreover, the three distinguished reservoir units contain hydrocarbons in different saturation ratios, and most of the hydrocarbons are residual (non-movable). Six different hydraulic flow units (HFU) can be recognized in the studied Unit A, depending on the variations in the porosity and permeability of the zones reflecting heterogeneity in the lithology or variations in the grain sizes. The N/G reservoir, pay, and productive ratios for the well BB-4 in Unit A under study are 9.2%, 3.28%, and 3.28%, respectively. The productive horizons are located in the RU-1.

Acknowledgments

The authors are very grateful to the Ministry of Natural Resources of the Kurdistan Region Government for their cooperation and for providing the data used in this study.

References

Al-Ameri, T. K., Al-Dolaimy, Q. H., & Al-Khafaji, A. J. (2009). Palynofacies and hydrocarbon generation potential of the upper Triassic Kurrachine Formation and lower part of the Baluti Formation, Mosul Block, Northwestern Iraq. *Arabian Journal of Geosciences*, *2*(3), 273–283. https://doi.org/10.1007/s12517-009-0041-5

Al-Ameri, T. K., & Zumberge, J. (2012). Middle and Upper Jurassic hydrocarbon potential of the Zagros Fold Belt, North Iraq. *Marine and Petroleum Geology*, *36*(1), 13–34. https://doi.org/10.1016/j.marpetgeo.2012.04.004

Al-Barzingy, S. J. (1999). *Source Rock Evaluation of Upper Triassic Kurra Chine Formation, Northwestern Iraq.* [Ph.D Dissertations]. Baghdad University of Baghdad.

Alhadithi, N. H. O., & Al-Hadithy, A. A. (2020). Differential Entrapment of Charged Hydrocarbon in Alan Field, Northern Iraq. *The Iraqi Geological Journal*, 68–76. https://doi.org/10.46717/igj.53.2A.5Rw-2020-08-05

Al-Sakini, J. (1992). *Summary of Petroleum Geology of Iraq and the Middle East. Internal Report in Arabic*.

Amaefule, J. O., Altunbay, M., Tiab, D., Kersey, D. G., & Keelan, D. K. (1993). Enhanced Reservoir Description: Using Core and Log Data to Identify Hydraulic (Flow) Units and Predict Permeability in Uncored Intervals/Wells. *SPE Annual Technical Conference and Exhibition*, SPE-26436-MS. https://doi.org/10.2118/26436-MS

Aqrawi, A. A. M., Goff, J. C., Horbury, A. D., & Sadooni, F. N. (2010). *Petroleum Geology of Iraq*. Scientific press Lt Po box 21, Beaconsfield, Bucks HP9 1NS, UK.

Asquith, G. B., & Gibosn, C. R. (1982). *Basic Well Log Analysis for Geologists*. American Association of Petroleum Geologists. https://doi.org/10.1306/Mth3425

Asquith, G. B., & Krygowski, D. (2004). Basic well log analysis. In *Methods in exploration series* (2. ed). AAPG.

Aswad, M. K., Omer, M. F., & Naqshabandi, S. F. (2024). Unlocking the hydrocarbon potential: Formation evaluation and petrophysical properties of the upper Triassic Kurra Chine Formation in Sarta Oil Field, Kurdistan Region, Northern Iraq. *Heliyon*, *10*(3), e25173. https://doi.org/10.1016/j.heliyon.2024.e25173

Awdal, A., Healy, D., & Alsop, G. I. (2016). Fracture patterns and petrophysical properties of carbonates undergoing regional folding: A case study from Kurdistan, N Iraq. *Marine and Petroleum Geology*, *71*, 149–167. https://doi.org/10.1016/j.marpetgeo.2015.12.017

Baban, D. H., & Ahmed, M. M. (2022a). Characterization of the Carbonate Reservoir Unit A of the Upper Triassic Kurra Chine Formation in the well SH-4, Shaikan Oilfield, Iraqi Kurdistan Region, Using Wireline Log Data. *Tikrit Journal of Pure Science*, *26*(2), 71–87. https://doi.org/10.25130/tjps.v26i2.122

Baban, D. H., & Ahmed, M. M. (2022b). Characterization of the Carbonate Reservoir Unit A of the Upper Triassic Kurra Chine Formation in the well SH-4, Shaikan Oilfield, Iraqi Kurdistan Region, Using Wireline Log Data. *Tikrit Journal of Pure Science*, *26*(2), 71–87. https://doi.org/10.25130/tjps.v26i2.122

Baban, D. H., Qadir, F., & Mohammed, A. (2020). Reservoir Rock Properties of the Upper Cretaceous Shiranish Formation in Taq Taq Oilfield, Iraqi Kurdistan Region. *Journal of Zankoy Sulaimani - Part A*, *22*(1), 363–388. https://doi.org/10.17656/jzs.10799

Baker Hughes. (1992). *Advanced Wire line and MWD Procedure Manual*.

Bassiouni, Z. (2008). Theory, measurement, and interpretation of well logs. In *SPE textbook series* (6. Nachdr.). Henry L. Doherty Memorial Fund of AIME, Soc. of Petroleum Engineers.

Bateman, R. M. (1985). *Open-hole log analysis and formation evaluation*. Reidel [u.a.].

Bellen, R. C. Van, Dunnington, H. V., Wetzel, R., & Morton, D. M. (1959). *Lexique stratigraphique international. Asie, Fascicule 10a, Iraq: Vol. Volume 10a*. Centre National de la Recherche Scientifique (CNRS), Paris.

Bowen, D. G. (2003). *Formation Evaluation and Petrophysics*.

Buday, T. (1980). *Stratigraphy and Paleontology" in The Regional Geology of Iraq: Vol. I*. Dar Al-Kutub Publishing House.

Cohen, K. M., Finney, S. C., Gibbard, P. L., & Fan, J.-X. (2013). The ICS International Chronostratigraphic Chart. *Episodes*, *36*(3), 199–204. https://doi.org/10.18814/epiiugs/2013/v36i3/002

Dallali, A. (2013). *Final report of the well Bina Bawi – 5*.

Darling, T. (2005). Well logging and formation evaluation. In *Gulf drilling guides*. Elsevier.

Dewan, J. T. (1983). *Essentials of modern open-hole log interpretation*. Pennwell Publ.

Dunnington, H. V. (1958). Generation, migration, accumulation, and dissipation of oil in northern Iraq. In *Habitat of Oil* (pp. 1194–1251). American Association of Petroleum Geologists (AAPG).

Edilbi, A. N. F., Kolo, K., Muhammed, N. R., Yasin, S. R., Mamaseni, W. J., & Akram, R. (2019). Source rock evaluation of shale intervals of the Kurra Chine Formation, Kurdistan Region-Iraq: An organic geochemical and basin modeling approach. *Egyptian Journal of Petroleum*, *28*(4), 315–321. https://doi.org/10.1016/j.ejpe.2019.06.003

Egbele, E., Ezuka, I., & Onyekonwu, M. (2005). Net-To-Gross Ratios: Implications in Integrated Reservoir Management Studies. *Nigeria Annual International Conference and Exhibition*, SPE-98808-MS. https://doi.org/10.2118/98808-MS

Ellis, D. V., & Singer, J. M. (2007). *Well Logging for Earth Scientists* (2 edition). Springer Netherlands. http://link.springer.com/10.1007/978-1-4020-4602-5

English, J. M., Lunn, G. A., Ferreira, L., & Yacu, G. (2015). Geologic evolution of the Iraqi Zagros, and its influence on the distribution of hydrocarbons in the Kurdistan region. *AAPG Bulletin*, *99*(02), 231–272. https://doi.org/10.1306/06271413205

Fea, I., Abioui, M., Nabawy, B. S., Jain, S., Bruno, D. Z., Kassem, A. A., & Benssaou, M. (2022). Reservoir quality discrimination of the Albian-Cenomanian reservoir sequences in the Ivorian basin: a lithological and petrophysical study. *Geomechanics and Geophysics for Geo-Energy and Geo-Resources*, *8*(1), 1. https://doi.org/10.1007/s40948-021-00297-8

Ghafur, A. A., Sissakian, V. K., Al-Ansari, N., Omer, H. O., & Abdulhaq, H. A. (2023). Tectonic development of northeastern part of the Arabian Plate: Examples from Pirmam and Bana Bawi anticlines in the Kurdistan region of north Iraq. *Results in Geophysical Sciences*, *14*, 100054. https://doi.org/10.1016/j.ringps.2023.100054

Ghorab, M., Ramadan, A. M., & Nouh, A. Z. (2008). The relation between shale origin (source or nonsource) and its type for Abu Roash Formation at Wadi-El Naturn area, south of Western Desert, Egypt. *Australian Journal of Basic Applied Sciences*, *2*(3), 360–371.

Gluyas, J., & Swarbrick, R. (2004). Petroleum Geosciences. *Blackwell Science Ltd. Hoboken*, 359.

Grunau, H. R. (1983). Abundance of Source Rocks for Oil and Gas Worldwide. *Journal of Petroleum Geology*, *6*(1), 39–53. https://doi.org/10.1111/j.1747-5457.1983.tb00261.x

Hamada, G. (2013). Identification of Hydrocarbon Movability and Type of Reservoir Fluids Using Resistivity Logs and Ratio of P-Wave Velocity/S-Wave Velocity (Vp/Vs). *SPE Asia Pacific Oil & Gas Conference and Exhibition*.

Hamood, O. (2012). *Geological Report for well Bina Bawi-3ST1*. Internal unpublished report. OMV Oil Company.

Hinsch, R., & Bretis, B. (2015). A semi-balanced section in the northwestern Zagros region: Constraining the structural architecture of the Mountain Front Flexure in the Kirkuk Embayment, Iraq. *GeoArabia*, *20*(4), 41–62. https://doi.org/10.2113/geoarabia200441

Jahn, F., Cook, M., & Graham, M. (2008). Hydrocarbon exploration and production. In *Developments in petroleum science* (2nd ed). Elsevier.

Jassim, S. Z., Buday, T., Cicha, I., & Prouza, V. (2006). Late Permian-Liassic Megasequence AP6. In Jassim S. Z. & J. C., Goff (Eds.), *Geology of Iraq, publication of Dolin, Prague and Moravian Museum, Brno: 341p.* (p. 431). , publication of Dolin, Prague and Moravian Museum.

Krygowsky, D. A. (2003). *Guide to Petrophysical Interpretation*, Texas, USA

Larionov, W. W. (1969). *Radiometrija Skwaschin*, Nedra, Moscow, U.S.S.R. Paper SPE26435.

Law, A., Megson, J., & Pye, M. (2001). Low permeability reservoirs: introduction. *Petroleum Geoscience*, *7*(1), 2–2. https://doi.org/10.1144/petgeo.7.1.2

Mackertich, D. S., & Samarrai, A. I. (2015). History of hydrocarbon exploration in the Kurdistan Region of Iraq. *GeoArabia*, *20*(2), 181–220. https://doi.org/10.2113/geoarabia2002181

Nelson, R.A. (2001) Geologic Analysis of Naturally Fractured Reservoirs. 2nd Edition, Gulf Professional Publishing, Boston, 332.
North, F. K. (1985). *Petroleum Geology*. Allen and Unwin Inc. Boston.
Parnell, J., Taylor, C. W., Thackrey, S., Osinski, G. R., & Lee, P. (2010). Permeability data for impact breccias imply focussed hydrothermal fluid flow. *Journal of Geochemical Exploration*, *106*(1–3), 171–175. https://doi.org/10.1016/j.gexplo.2009.12.002
Peters, E. J. (2001). *Advanced Petrophysics,* University of Texas, Austin TX.
Ryder Scott Company. (2011). *Estimated unrisked discovered and undiscovered total petroleum initially in place attributable to certain interests in the Shaikan License Block, Kurdistan, Iraq.*
Sadooni, F. N. (1995). Petroleum Prospects of Upper Triassic Carbonates in Northern Iraq. *Journal of Petroleum Geology*, *18*(2), 171–190.
https://doi.org/10.1111/j.1747-5457.1995.tb00896.x
Sadooni, F. N., & Alsharhan, A. S. (2004). Stratigraphy, lithofacies distribution, and petroleum potential of the Triassic strata of the northern Arabian plate. *AAPG Bulletin*, *88*(4), 515–538. https://doi.org/10.1306/12030303067
Schlumberger. (1972). *Log Interpretation / Charts:* (Vol. 1). Schlumberger Well Services Inc.
Schlumberger. (1989). *Log Interpretation Principles/Applications*. Schlumberger Educational Services.
Thomas, E. C., & Stieber, S. J. (1975). The distribution of shale in sandstones and its effect upon porosity. *New York, USA.*
Tiab, D. (2000). *Advances in petrophysics, Vol. 1—flow units.* Lecture notes manual, University of Oklahoma.
Tiab, D., & Donaldson, E. C. (2012). *Petrophysics: theory and practice of measuring reservoir rock and fluid transport properties* (3rd ed). Gulf Professional Pub.
Vulama, I. (2011). Source Rock Generative Potential and Volumetric Characteristics of the Kurra Chine Dolomite Formation, Hayan Block, Central Syrian Palmerides. *Geologia Croatica, 64(3), 259-272.*, *64*(3), 259–272.
Yang, L. (2015). *A Petrophysical Evaluation of the Trenton-Black River Formation of the Michigan Basin*. https://digitalcommons.mtu.edu/etds/914
Zebari, M. (2013). *Geometry and evolution of fold structures within the High Folded Zone: Zagros Fold-Thrust Belt, Kurdistan Region-Iraq.* MSc Thesis, University of Nebraska-Lincoln.

About the authors

Dler H. Baban (Ph.D.) is a professor of petroleum geology at the Department of Earth Sciences and Petroleum at the University of Sulaimani. Dler earned his M.Sc. in general geology from the Department of Geology/ University of Baghdad in 1989 and his Ph.D. in petroleum geology in 1996 from the same department. Dler supervised a number of M.Sc. and Ph.D. students in petroleum geology specifications and worked as a consultant for the FAO organization and for a number of foreign oil companies in the southern Kurdistan Region.

e-mail: dler.mohamad@univsul.edu.iq

Mustafa M. Nanakali graduated from the Department of Petroleum Geosciences at the University of Soran in 2016 and was hired as a demonstrator in the Center of Scientific Research at the same university in 2017. Mustafa earned his M.Sc. degree in Petroleum Geology from the Department of Geology at the University of Sulaimani in 2023, and he is currently a Ph.D. student in the Department of Petroleum Geosciences at the University of Soran.

e-mail: geopetrol1995@gmail.com